Reduced-Bandwidth and Distributed MWF-Based Noise Reduction Algorithms for Binaural Hearing Aids

Simon Doclo, *Member, IEEE*, Marc Moonen, *Fellow, IEEE*, Tim Van den Bogaert, *Member, IEEE*, and Jan Wouters

***Abstract*—In a binaural hearing aid system, output signals need to be generated for the left and the right ear. Using the binaural multichannel Wiener filter (MWF), which exploits all microphone signals from both hearing aids, a significant reduction of background noise can be achieved. However, due to power and bandwidth limitations of the binaural link, it is typically not possible to transmit all microphone signals between the hearing aids. To limit the amount of transmitted information, this paper presents reduced-bandwidth MWF-based noise reduction algorithms, where a filtered combination of the contralateral microphone signals is transmitted. A first scheme uses a signal-independent beamformer, whereas a second scheme uses the output of a monaural MWF on the contralateral microphone signals and a third scheme involves an iterative distributed MWF (DB-MWF) procedure. It is shown that in the case of a rank-1 speech correlation matrix, corresponding to a single speech source, the DB-MWF procedure converges to the binaural MWF solution. Experimental results compare the noise reduction performance of the reduced-bandwidth algorithms with respect to the benchmark binaural MWF. It is shown that the best performance of the reduced-bandwidth algorithms is obtained by the DB-MWF procedure and that the performance of the DB-MWF procedure approaches quite well the optimal performance of the binaural MWF.**

***Index Terms*—Binaural hearing aid, distributed processing, multichannel Wiener filter (MWF), noise reduction.**

Manuscript received September 20, 2007; revised April 28, 2008. Current version published December 11, 2008. This work was carried out at the ESAT-SCD and ExpORL laboratories of Katholieke Universiteit Leuven, Belgium, and was supported in part by the IWT Project (Improving the perception of speech and music in cochlear implants), by the Concerted Research Action GOA-AMBIORICS (Algorithms for medical and biological research, integration, computation, and software), by the K.U.Leuven Research Council CoE EF/05/006 (Optimization in Engineering), and by the Interuniversity Attraction Pole IAP P6/04 DYSCO (Dynamical systems, control, and optimization), initiated by the Belgian Federal Science Policy Office. The associate editor coordinating the review of this manuscript and approving it for publication was Dr. Sylvain Marchand.

S. Doclo was with the Department of Electrical Engineering (ESAT–SCD), Katholieke Universiteit Leuven, B-3001 Leuven, Belgium. He is now with the Sounds and Systems Group, NXP Semiconductors, B-3001 Leuven, Belgium (e-mail: simon.doclo@esat.kuleuven.be).

M. Moonen is with the Department of Electrical Engineering (ESAT–SCD), Katholieke Universiteit Leuven, B-3001 Leuven, Belgium (e-mail: marc.moonen@esat.kuleuven.be).

T. Van den Bogaert and J. Wouters are with the Department of Neurosciences, ExpORL, Katholieke Universiteit Leuven, 3000 Leuven, Belgium (e-mail: tim.vandenbogaert@med.kuleuven.be; jan.wouters@med.kuleuven.be).

Color versions of one or more of the figures in this paper are available online at http://ieeexplore.ieee.org.

Digital Object Identifier 10.1109/TASL.2008.2004291

I. Introduction

NOISE reduction algorithms in hearing aids are crucial to improve speech understanding in background noise for hearing-impaired persons. Since multimicrophone noise reduction systems are able to exploit spatial information in addition to spectro–temporal information, they are typically preferred to single-microphone systems. In a dual hearing aid system, output signals for both ears are generated, either by operating both hearing aids independently (a bilateral system) or by sharing information between the hearing aids (a binaural system) [1]–[10], e.g., using a wireless link.

In [11], a binaural multichannel Wiener filter (MWF) technique has been proposed that produces an estimate of the desired speech signal component in both hearing aids and that enables a tradeoff between noise reduction and speech distortion. It has been shown that this technique—and its extensions—provides significant noise reduction and is able to partly preserve the binaural localization cues, i.e., the interaural time and level difference [11]–[14], [25]. This binaural MWF will be reviewed in Section III. Since the binaural MWF optimally exploits all microphone signals from both hearing aids, all microphone signals need to be transmitted over the binaural link, requiring a large bandwidth.

Currently available binaural hearing aids with a wireless link have very limited data rates (e.g., 215 bit/s [15]) and are only able to transmit data in order to compare and coordinate the parameter settings of both hearing aids (e.g., volume, acoustic scene classification, noise reduction parameters). Although future binaural hearing aids will also allow for transmission of (coded) audio signals [16], power consumption will severely restrict the number of microphone signals that can be transmitted. Hence, Section IV presents reduced-bandwidth MWF-based noise reduction algorithms where only one signal is transmitted from the contralateral side. First, suboptimal schemes are discussed, either using the front contralateral microphone signal, using a signal-independent superdirective beamformer or using the output of a monaural MWF on the contralateral microphone signals. Next, an iterative distributed MWF (DB-MWF) procedure is presented that—remarkably—converges to the binaural MWF solution in the case of a rank-1 speech correlation matrix and that approaches the binaural MWF solution if this rank-1 property is not satisfied.

For a binaural hearing aid system with two microphones on each hearing aid, Section V compares the performance of all discussed binaural noise reduction algorithms for several realistic speech and noise configurations and for different reverberation conditions. In general, the binaural MWF results in

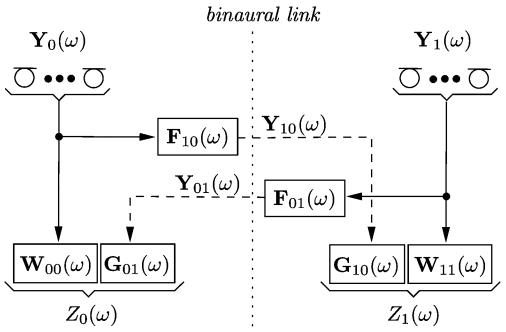

Fig. 1. General binaural processing scheme.

the largest SNR improvement and the best performance of the considered reduced-bandwidth algorithms is achieved by the DB-MWF procedure. For most configurations, the performance of the DB-MWF procedure moreover approaches the performance of the binaural MWF, even though the speech correlation matrices in the simulations are not rank-1 matrices. It is also shown that the iterative DB-MWF procedure already converges after two or three iterations. In addition, Section V investigates the influence of the fast Fourier transform (FFT) size on the performance and analyzes the contralateral spatial directivity pattern, showing that optimally a signal with a high SNR should be transmitted from the contralateral side.

II. Configuration and Notation

We consider the binaural hearing aid configuration depicted in Fig. 1, where both hearing aids have a microphone array consisting of M microphones. The mth microphone signal in the left hearing aid $Y_{0,m}(\omega)$ can be written in the frequency-domain as

$$Y_{0,m}(\omega) = X_{0,m}(\omega) + V_{0,m}(\omega), \quad m = 0 \dots M-1 \tag{1}$$

where $X_{0,m}(\omega)$ represents the speech component and $V_{0,m}(\omega)$ represents the noise component. Similarly, the mth microphone signal in the right hearing aid is $Y_{1,m}(\omega) = X_{1,m}(\omega)+V_{1,m}(\omega)$. For conciseness we will omit the frequency-domain variable ω from now on.

We define the M-dimensional stacked vectors $\mathbf{Y}_0$ and $\mathbf{Y}_1$ and the $2M$-dimensional signal vector $\mathbf{Y}$ as

$$\mathbf{Y}_0 = \begin{bmatrix} Y_{0,0} \\ \vdots \\ Y_{0,M-1} \end{bmatrix} \quad \mathbf{Y}_1 = \begin{bmatrix} Y_{1,0} \\ \vdots \\ Y_{1,M-1} \end{bmatrix} \quad \mathbf{Y} = \begin{bmatrix} \mathbf{Y}_0 \\ \mathbf{Y}_1 \end{bmatrix}. \tag{2}$$

The signal vector can be written as $\mathbf{Y} = \mathbf{X} + \mathbf{V}$, where $\mathbf{X}$ and $\mathbf{V}$ are defined similarly to $\mathbf{Y}$.

In the case of a *single speech source*, the speech signal vector can be written as

$$\mathbf{X} = \mathbf{A}S \tag{3}$$

with the $2M$-dimensional steering vector $\mathbf{A}$ containing the acoustic transfer functions from the speech source to the microphones (including room acoustics, microphone characteristics, and head shadow effect) and S the speech signal. The vector $\mathbf{A}$ is defined similarly to $\mathbf{Y}$ in (2), i.e.,

$$\mathbf{A} = \begin{bmatrix} \mathbf{A}_0 \\ \mathbf{A}_1 \end{bmatrix} \quad \mathbf{A}_0 = \begin{bmatrix} A_{0,0} \\ \vdots \\ A_{0,M-1} \end{bmatrix} \quad \mathbf{A}_1 = \begin{bmatrix} A_{1,0} \\ \vdots \\ A_{1,M-1} \end{bmatrix}. \tag{4}$$

In a binaural processing scheme, collaboration between both hearing aids is achieved by transmitting signals between the hearing aids (e.g., using a wireless link). The signals transmitted from the left hearing aid to the right hearing aid are represented by the N-dimensional vector $\mathbf{Y}_{10}$, and the signals transmitted from the right hearing aid to the left hearing aid are represented by the N-dimensional vector $\mathbf{Y}_{01}$, typically with $N \leq M$. We assume that the transmitted signals are a linear combination of the contralateral microphone signals, i.e.,

$$\mathbf{Y}_{10} = \mathbf{F}_{10}^H \mathbf{Y}_0, \quad \mathbf{Y}_{01} = \mathbf{F}_{01}^H \mathbf{Y}_1 \tag{5}$$

where $\mathbf{F}_{10}$ and $\mathbf{F}_{01}$ are $M \times N$-dimensional complex matrices.

The output signals Z_0 and Z_1 for the left and the right ear are obtained by filtering and summing the ipsilateral microphone signals and the transmitted signals from the contralateral ear, i.e.,

$$Z_0 = \mathbf{W}_{00}^H \mathbf{Y}_0 + \mathbf{G}_{01}^H \mathbf{Y}_{01} = \mathbf{W}_{00}^H \mathbf{Y}_0 + \mathbf{G}_{01}^H \mathbf{F}_{01}^H \mathbf{Y}_1 \tag{6}$$

$$Z_1 = \mathbf{G}_{10}^H \mathbf{Y}_{10} + \mathbf{W}_{11}^H \mathbf{Y}_1 = \mathbf{G}_{10}^H \mathbf{F}_{10}^H \mathbf{Y}_0 + \mathbf{W}_{11}^H \mathbf{Y}_1 \tag{7}$$

where $\mathbf{W}_{00}$ and $\mathbf{W}_{11}$ are M-dimensional vectors and $\mathbf{G}_{01}$ and $\mathbf{G}_{10}$ are N-dimensional vectors. Hence, the output signals can be written as linear combinations of all microphone signals, i.e.,

$$Z_0 = \mathbf{W}_0^H \mathbf{Y}, \quad Z_1 = \mathbf{W}_1^H \mathbf{Y} \tag{8}$$

where the $2M$-dimensional vectors $\mathbf{W}_0$ and $\mathbf{W}_1$ are given as

$$\mathbf{W}_0 = \begin{bmatrix} \mathbf{W}_{00} \\ \mathbf{W}_{01} \end{bmatrix} = \begin{bmatrix} \mathbf{W}_{00} \\ \mathbf{F}_{01}\mathbf{G}_{01} \end{bmatrix}$$
$$\mathbf{W}_1 = \begin{bmatrix} \mathbf{W}_{10} \\ \mathbf{W}_{11} \end{bmatrix} = \begin{bmatrix} \mathbf{F}_{10}\mathbf{G}_{10} \\ \mathbf{W}_{11} \end{bmatrix}. \tag{9}$$

III. Binaural Multichannel Wiener Filter

The binaural MWF in [11] assumes that all microphone signals are transmitted, i.e., $\mathbf{F}_{10} = \mathbf{F}_{01} = \mathbf{I}_M$, with $\mathbf{I}_M$ the $M \times M$-dimensional identity matrix. The binaural MWF produces a minimum-mean-square-error (MMSE) estimate of the speech component in both hearing aids, hence simultaneously performing noise reduction and limiting speech distortion. The MSE cost function for the filter $\mathbf{W}_0$, estimating the speech component $X_{0,0}$ in the front microphone of the left hearing aid, is equal to

$$\begin{aligned} J_{MSE,0}(\mathbf{W}_0) &= \mathcal{E}\left\{|X_{0,0} - \mathbf{W}_0^H \mathbf{Y}|^2\right\} \\ &= \mathcal{E}\left\{|X_{0,0} - \mathbf{W}_0^H \mathbf{X}|^2\right\} + \mathcal{E}\left\{|\mathbf{W}_0^H \mathbf{V}|^2\right\} \end{aligned} \tag{10}$$

where we have assumed statistical independence between the speech component $\mathbf{X}$ and the noise component $\mathbf{V}$. Alternatively,

to provide a tradeoff between speech distortion and noise reduction, the speech distortion weighted multichannel Wiener filter (SDW-MWF) minimizes the weighted sum of the residual noise energy and the speech distortion energy [17], [18], i.e.,

$$\boxed{J_0(\mathbf{W}_0) = \mathcal{E}\left\{|X_{0,0} - \mathbf{W}_0^H\mathbf{X}|^2\right\} + \mu\mathcal{E}\left\{|\mathbf{W}_0^H\mathbf{V}|^2\right\}} \quad (11)$$

where μ is the tradeoff parameter. Similarly, the SDW-MWF cost function for the filter $\mathbf{W}_1$ estimating the speech component $X_{1,0}$ in the front microphone of the right hearing aid is equal to

$$\boxed{J_1(\mathbf{W}_1) = \mathcal{E}\left\{|X_{1,0} - \mathbf{W}_1^H\mathbf{X}|^2\right\} + \mu\mathcal{E}\left\{|\mathbf{W}_1^H\mathbf{V}|^2\right\}}. \quad (12)$$

In the following, we will use SDW-MWF cost functions (and algorithms), but for conciseness refer to these as MWF cost functions (and algorithms).

Defining $\mathbf{R}_x$ and $\mathbf{R}_v$ as the $2M \times 2M$-dimensional speech and the noise correlation matrices, i.e.,

$$\mathbf{R}_x = \mathcal{E}\{\mathbf{X}\mathbf{X}^H\}, \quad \mathbf{R}_v = \mathcal{E}\{\mathbf{V}\mathbf{V}^H\} \quad (13)$$

the MWF cost functions can be written as

$$\begin{aligned} J_0(\mathbf{W}_0) &= P_0 - \mathbf{r}_{x0}^H\mathbf{W}_0 - \mathbf{W}_0^H\mathbf{r}_{x0} \\ &\quad + \mathbf{W}_0^H(\mathbf{R}_x + \mu\mathbf{R}_v)\mathbf{W}_0 \quad (14) \\ J_1(\mathbf{W}_1) &= P_1 - \mathbf{r}_{x1}^H\mathbf{W}_1 - \mathbf{W}_1^H\mathbf{r}_{x1} \\ &\quad + \mathbf{W}_1^H(\mathbf{R}_x + \mu\mathbf{R}_v)\mathbf{W}_1 \quad (15) \end{aligned}$$

with

$$P_0 = \mathcal{E}\left\{|X_{0,0}|^2\right\} \quad \mathbf{r}_{x0} = \mathcal{E}\{\mathbf{X}X_{0,0}^*\} = \mathbf{R}_x\mathbf{e}_0 \quad (16)$$

$$P_1 = \mathcal{E}\left\{|X_{1,0}|^2\right\} \quad \mathbf{r}_{x1} = \mathcal{E}\{\mathbf{X}X_{1,0}^*\} = \mathbf{R}_x\mathbf{e}_1. \quad (17)$$

The vectors $\mathbf{e}_0$ and $\mathbf{e}_1$ are $2M$-dimensional vectors with only one element equal to 1 and the other elements equal to 0, and with $\mathbf{e}_0(1) = 1$ and $\mathbf{e}_1(M+1) = 1$. In practice, the speech correlation matrix $\mathbf{R}_x$ obviously is unknown, but it can be estimated as $\mathbf{R}_x = \mathbf{R}_y - \mathbf{R}_v$, with $\mathbf{R}_y = \mathcal{E}\{\mathbf{Y}\mathbf{Y}^H\}$. The noise correlation matrix $\mathbf{R}_v$ can be computed during noise-only periods and the correlation matrix $\mathbf{R}_y$ can be computed during speech-and-noise periods, requiring a voice activity detection mechanism.

The binaural MWF cost function is obtained by summing the (independent) cost functions for the left and the right hearing aid in (11) and (12), i.e.,

$$\boxed{J(\mathbf{W}) = J_0(\mathbf{W}_0) + J_1(\mathbf{W}_1) = P - \mathbf{r}_x^H\mathbf{W} - \mathbf{W}^H\mathbf{r}_x + \mathbf{W}^H\mathbf{R}\mathbf{W}} \quad (18)$$

with $P = P_0 + P_1$, and the $4M$-dimensional vectors $\mathbf{W}$ and $\mathbf{r}_x$ and the $4M \times 4M$-dimensional matrix $\mathbf{R}$ defined as

$$\mathbf{W} = \begin{bmatrix} \mathbf{W}_0 \\ \mathbf{W}_1 \end{bmatrix}, \quad \mathbf{r}_x = \begin{bmatrix} \mathbf{r}_{x0} \\ \mathbf{r}_{x1} \end{bmatrix}$$

$$\mathbf{R} = \begin{bmatrix} \mathbf{R}_x + \mu\mathbf{R}_v & \mathbf{0} \\ \mathbf{0} & \mathbf{R}_x + \mu\mathbf{R}_v \end{bmatrix}. \quad (19)$$

Assuming $\mathbf{R}_v$ is a positive definite matrix and $\mu > 0$, the matrix $\mathbf{R}$ is a positive definite matrix.

By setting the gradient of $J(\mathbf{W})$ with respect to $\mathbf{W}$ equal to zero, the filter $\mathbf{W}^m$ minimizing (18) is equal to

$$\mathbf{W}^m = \mathbf{R}^{-1}\mathbf{r}_x \quad (20)$$

such that using (16), (17), and (19), the optimal filters $\mathbf{W}_0^m$ and $\mathbf{W}_1^m$ are given as

$$\boxed{\mathbf{W}_0^m = (\mathbf{R}_x + \mu\mathbf{R}_v)^{-1}\mathbf{R}_x\mathbf{e}_0, \quad \mathbf{W}_1^m = (\mathbf{R}_x + \mu\mathbf{R}_v)^{-1}\mathbf{R}_x\mathbf{e}_1} \quad (21)$$

and the minima of the MWF cost functions are equal to

$$J_0(\mathbf{W}_0^m) = \mathbf{e}_0^H\mathbf{R}_x\mathbf{e}_0 - \mathbf{e}_0^H\mathbf{R}_x(\mathbf{R}_x + \mu\mathbf{R}_v)^{-1}\mathbf{R}_x\mathbf{e}_0 \quad (22)$$

$$J_1(\mathbf{W}_1^m) = \mathbf{e}_1^H\mathbf{R}_x\mathbf{e}_1 - \mathbf{e}_1^H\mathbf{R}_x(\mathbf{R}_x + \mu\mathbf{R}_v)^{-1}\mathbf{R}_x\mathbf{e}_1. \quad (23)$$

In the case of a *single speech source*, the speech correlation matrix is a rank-1 matrix, i.e.,

$$\mathbf{R}_x = P_s\mathbf{A}\mathbf{A}^H \quad (24)$$

with $P_s = \mathcal{E}\{|S|^2\}$ the power of the speech signal. Using the matrix inversion lemma, the filters $\mathbf{W}_0^m$ and $\mathbf{W}_1^m$ are then found to be equal to

$$\boxed{\mathbf{W}_0^m = \frac{\mathbf{R}_v^{-1}\mathbf{A}}{\mathbf{A}^H\mathbf{R}_v^{-1}\mathbf{A} + \frac{\mu}{P_s}}A_{0,0}^*, \quad \mathbf{W}_1^m = \frac{\mathbf{R}_v^{-1}\mathbf{A}}{\mathbf{A}^H\mathbf{R}_v^{-1}\mathbf{A} + \frac{\mu}{P_s}}A_{1,0}^*} \quad (25)$$

with $A_{0,0}$ and $A_{1,0}$ elements of $\mathbf{A}$, cf. (4). This implies that

$$\boxed{\mathbf{W}_1^m = \alpha\mathbf{W}_0^m} \quad (26)$$

where

$$\alpha = \frac{A_{1,0}^*}{A_{0,0}^*} = \frac{X_{1,0}^*}{X_{0,0}^*} \quad (27)$$

is the complex conjugate of the interaural transfer function (ITF) [13], [14] of the speech component. Hence, in the case of a single speech source the binaural MWF filter vectors for the left and the right hearing aid are *parallel*, which in general is not the case for (21). In the case of a single speech source, the minima of the MWF cost functions are equal to

$$\begin{aligned} J_0(\mathbf{W}_0^m) &= \frac{\mu|A_{0,0}|^2}{\mathbf{A}^H\mathbf{R}_v^{-1}\mathbf{A} + \frac{\mu}{P_s}} \\ J_1(\mathbf{W}_1^m) &= \frac{\mu|A_{1,0}|^2}{\mathbf{A}^H\mathbf{R}_v^{-1}\mathbf{A} + \frac{\mu}{P_s}} \quad (28) \end{aligned}$$

such that $J_1(\mathbf{W}_1^m) = |\alpha|^2 J_0(\mathbf{W}_0^m)$.

IV. Reduced-Bandwidth MWF Algorithms

The binaural MWF (B-MWF) discussed in Section III exploits all microphone signals, requiring $2N = 2M$ signals to be transmitted over the binaural link. In order to limit power consumption (and bandwidth), this section presents MWF-based algorithms that use only one signal transmitted from the contralat-

eral ear, i.e., $N = 1$, reducing $\mathbf{F}_{01}$ and $\mathbf{F}_{10}$ to M-dimensional vectors and $\mathbf{G}_{01}$ and $\mathbf{G}_{10}$ to scalars, i.e.,

$$\mathbf{W}_0 = \begin{bmatrix} \mathbf{W}_{00} \\ G_{01}\mathbf{F}_{01} \end{bmatrix}, \quad \mathbf{W}_1 = \begin{bmatrix} G_{10}\mathbf{F}_{10} \\ \mathbf{W}_{11} \end{bmatrix}. \tag{29}$$

This corresponds to constraining $\mathbf{W}_{01}$ to be parallel to $\mathbf{F}_{01}$ and $\mathbf{W}_{10}$ to be parallel to $\mathbf{F}_{10}$. It is important to observe that the B-MWF in (21) can still be obtained using this scheme, namely if $\mathbf{F}_{01}$ is parallel to $\mathbf{W}_{01}^m$ and $\mathbf{F}_{10}$ is parallel to $\mathbf{W}_{10}^m$. However, these filters now have to be computed without all microphone signals being transmitted, which seems infeasible at first sight since the full correlation matrices in (13) can not be computed.

Sections IV-A and IV-B first present *suboptimal schemes*, either using (signal-independent) fixed beamformers or using the (signal-dependent) output of a monaural MWF on the contralateral microphone signals. In Section IV-C an *iterative distributed MWF procedure* is presented that converges to the B-MWF solution in the case of a rank-1 speech correlation matrix and that approaches the B-MWF solution if this rank-1 property is not satisfied.

A. Fixed Beamformer (MWF-Front and MWF-Superd)

In this scheme, the filters $\mathbf{F}_{01}$ and $\mathbf{F}_{10}$, which can be viewed as monaural beamformers, are signal-independent. In a simple implementation, only the contralateral front microphone signals are transmitted, i.e., $\mathbf{F}_{01} = \mathbf{F}_{10} = [1 \quad 0 \quad \dots \quad 0]^T$ (MWF-front), whereas in a more advanced implementation $\mathbf{F}_{01}$ and $\mathbf{F}_{10}$ are monaural superdirective beamformers (MWF-superd). Section V-A explains in more detail how these superdirective beamformers are computed.

B. Contralateral MWF (MWF-Contra)

In this scheme, the transmitted signals are the output of a monaural MWF, estimating the contralateral speech component only using the M contralateral microphone signals. Hence, the filters $\mathbf{F}_{01}$ and $\mathbf{F}_{10}$ can be found as

$$\begin{aligned} \mathbf{F}_{01} = \arg\min_{\mathbf{F}} \mathcal{E}\left\{|X_{1,0} - \mathbf{F}^H\mathbf{X}_1|^2\right\} \\ + \mu\mathcal{E}\left\{|\mathbf{F}^H\mathbf{V}_1|^2\right\} \end{aligned} \tag{30}$$

$$\begin{aligned} \mathbf{F}_{10} = \arg\min_{\mathbf{F}} \mathcal{E}\left\{|X_{0,0} - \mathbf{F}^H\mathbf{X}_0|^2\right\} \\ + \mu\mathcal{E}\left\{|\mathbf{F}^H\mathbf{V}_0|^2\right\}. \end{aligned} \tag{31}$$

The resulting filters can be written, using $\mathbf{Q}_0 = [\mathbf{I}_M \quad \mathbf{0}_M]$ and $\mathbf{Q}_1 = [\mathbf{0}_M \quad \mathbf{I}_M]$, as

$$\mathbf{F}_{01} = \left[\mathbf{Q}_1(\mathbf{R}_x + \mu\mathbf{R}_v)\mathbf{Q}_1^T\right]^{-1}\mathbf{Q}_1\mathbf{R}_x\mathbf{e}_1 \tag{32}$$

$$\mathbf{F}_{10} = \left[\mathbf{Q}_0(\mathbf{R}_x + \mu\mathbf{R}_v)\mathbf{Q}_0^T\right]^{-1}\mathbf{Q}_0\mathbf{R}_x\mathbf{e}_0. \tag{33}$$

In Appendix A, it is shown that in general this scheme is *suboptimal*, since $\mathbf{F}_{01}$ is not parallel to $\mathbf{W}_{01}^m$ and $\mathbf{F}_{10}$ is not parallel to $\mathbf{W}_{10}^m$. It is also shown that the optimal B-MWF solution is obtained in the case of a single speech source and when the noise components between the left and the right hearing aid are uncorrelated. However, since this scenario does not occur in practice, we expect the MWF-contra performance always to be lower than the B-MWF performance, which is verified by the experimental results in Section V. In addition, the MWF-contra scheme has a high computational complexity, since two MWF solutions now have to be computed on each hearing aid, e.g., for the left hearing aid an M-dimensional MWF for computing $\mathbf{F}_{10}$ and an $(M+1)$-dimensional MWF for computing $\mathbf{W}_{00}$ and G_{01}.

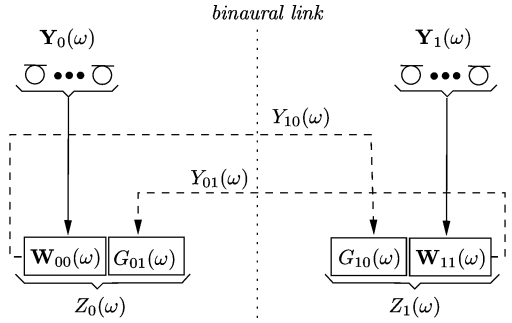

Fig. 2. Distributed binaural MWF procedure (DB-MWF).

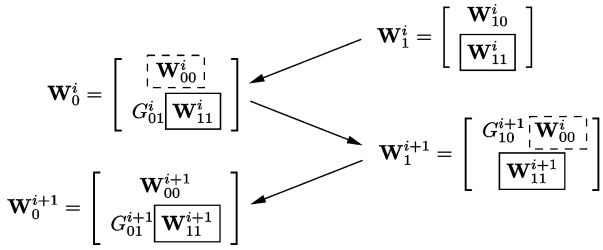

Fig. 3. Iterative procedure for updating the filter coefficients at the left and the right hearing aid.

C. Iterative Distributed Binaural MWF Procedure (DB-MWF)

The distributed binaural MWF scheme is depicted in Fig. 2. Basically, in each iteration the filter $\mathbf{F}_{10}$ is equal to $\mathbf{W}_{00}$ from the previous iteration, and the filter $\mathbf{F}_{01}$ is equal to $\mathbf{W}_{11}$ from the previous iteration. If we denote the filters and the signals in the ith iteration with superscript i, then the iterative procedure runs as follows (see Figs. 2 and 3).

1) Transmit $Y_{01}^i = \mathbf{F}_{01}^{i,H}\mathbf{Y}_1$ to the left hearing aid, with $\mathbf{F}_{01}^i = \mathbf{W}_{11}^i$.
2) Using $\mathbf{Y}_0$ and Y_{01}^i as input signals, calculate $\mathbf{W}_{00}^i$ and G_{01}^i that minimize the MWF cost function estimating the speech component in the left front microphone, i.e.,

$$\begin{aligned} J_0^i(\mathbf{W}_{00}, G_{01}) = \mathcal{E}\left\{|X_{0,0} - (\mathbf{W}_{00}^H\mathbf{X}_0 + G_{01}^* X_{01}^i)|^2\right\} \\ + \mu\mathcal{E}\left\{|\mathbf{W}_{00}^H\mathbf{V}_0 + G_{01}^* V_{01}^i|^2\right\}. \end{aligned} \tag{34}$$

3) Transmit $Y_{10}^{i+1} = \mathbf{F}_{10}^{i+1,H}\mathbf{Y}_0$ to the right hearing aid, with $\mathbf{F}_{10}^{i+1} = \mathbf{W}_{00}^i$.
4) Using $\mathbf{Y}_1$ and Y_{10}^{i+1} as input signals, calculate $\mathbf{W}_{11}^{i+1}$ and G_{10}^{i+1} that minimize the MWF cost function estimating the speech component in the right front microphone, i.e.,

$$\begin{aligned} J_1^{i+1}(\mathbf{W}_{11}, G_{10}) = \mathcal{E}\left\{|X_{1,0} - \left(\mathbf{W}_{11}^H\mathbf{X}_1 + G_{10}^* X_{10}^{i+1}\right)|^2\right\} \\ + \mu\mathcal{E}\left\{\left|\mathbf{W}_{11}^H\mathbf{V}_1 + G_{10}^* V_{10}^{i+1}\right|^2\right\}. \end{aligned} \tag{35}$$

Hence, considering (29), the $2M$-dimensional filters $\mathbf{W}_0^i$ and $\mathbf{W}_1^{i+1}$ are structured as

$$\mathbf{W}_0^i = \begin{bmatrix} \mathbf{W}_{00}^i \\ G_{01}^i\mathbf{W}_{11}^i \end{bmatrix}, \quad \mathbf{W}_1^{i+1} = \begin{bmatrix} G_{10}^{i+1}\mathbf{W}_{00}^i \\ \mathbf{W}_{11}^{i+1} \end{bmatrix} \tag{36}$$

which is also depicted in Fig. 3. Hence, if the procedure converges (see below), then the following relationship holds for $i \rightarrow \infty$:

$$\boxed{\begin{bmatrix} \mathbf{W}_{10}^{\infty} \\ \mathbf{W}_{11}^{\infty} \end{bmatrix} = \begin{bmatrix} G_{10}^{\infty}\mathbf{W}_{00}^{\infty} \\ \frac{1}{G_{01}^{\infty}}\mathbf{W}_{01}^{\infty} \end{bmatrix}} \tag{37}$$

i.e., the first (second) part of $\mathbf{W}_1^{\infty}$ is parallel to the first (second) part of $\mathbf{W}_0^{\infty}$.

We now show that in the case of a *single speech source*, the iterative DB-MWF procedure—remarkably—converges to the B-MWF solution in (25). First, it is shown that the MWF cost function in (18) decreases in each iteration of the DB-MWF procedure, i.e.,

$$\boxed{J\left(\begin{bmatrix} \mathbf{W}_0^{i+1} \\ \mathbf{W}_1^{i+1} \end{bmatrix}\right) \leq J\left(\begin{bmatrix} \mathbf{W}_0^{i} \\ \mathbf{W}_1^{i} \end{bmatrix}\right)} \tag{38}$$

In particular, we will prove that

$$J_0\left(\mathbf{W}_0^{i+1}\right) \leq J_0\left(\mathbf{W}_0^{i}\right), \quad J_1\left(\mathbf{W}_1^{i+1}\right) \leq J_1\left(\mathbf{W}_1^{i}\right). \tag{39}$$

Proof: In the case of a single speech source, the MWF cost functions in (11) and (12) are equal to

$$\begin{aligned} J_0(\mathbf{W}_0) &= P_s\,\mathcal{E}\left\{|A_{0,0} - \mathbf{W}_0^H\mathbf{A}|^2\right\} \\ &\quad + \mu\mathcal{E}\left\{|\mathbf{W}_0^H\mathbf{V}|^2\right\} \end{aligned} \tag{40}$$

$$\begin{aligned} J_1(\mathbf{W}_1) &= P_s\mathcal{E}\left\{|A_{1,0} - \mathbf{W}_1^H\mathbf{A}|^2\right\} \\ &\quad + \mu\mathcal{E}\left\{|\mathbf{W}_1^H\mathbf{V}|^2\right\} \end{aligned} \tag{41}$$

such that, using $\alpha = A_{1,0}^*/A_{0,0}^*$ defined in (27), the following relationships hold for any $\mathbf{W}_0$ and $\mathbf{W}_1$:

$$\begin{aligned} J_0\left(\frac{\mathbf{W}_0}{\alpha}\right) &= P_s\,\mathcal{E}\left\{\left|\frac{A_{0,0}\,\alpha^* - \mathbf{W}_0^H\mathbf{A}}{\alpha^*}\right|^2\right\} + \mu\mathcal{E}\left\{\left|\frac{\mathbf{W}_0^H\mathbf{V}}{\alpha^*}\right|^2\right\} \\ &= \frac{J_1(\mathbf{W}_0)}{|\alpha|^2} \end{aligned} \tag{42}$$

$$\begin{aligned} J_1(\alpha\mathbf{W}_1) &= P_s\mathcal{E}\left\{\left|\alpha^*\left(\frac{A_{1,0}}{\alpha^*} - \mathbf{W}_1^H\mathbf{A}\right)\right|^2\right\} + \mu\mathcal{E}\left\{|\alpha^*\mathbf{W}_1^H\mathbf{V}|^2\right\} \\ &= |\alpha|^2 J_0(\mathbf{W}_1). \end{aligned} \tag{43}$$

Since $\mathbf{W}_{00}^i$ and G_{01}^i minimize J_0^i in (34), it readily follows that

$$J_0(\mathbf{W}_0^i) = J_0^i(\mathbf{W}_{00}^i, G_{01}^i) \leq J_0^i\left(\frac{\mathbf{W}_{10}^i}{\alpha}, \frac{1}{\alpha}\right) = J_0\left(\frac{\mathbf{W}_1^i}{\alpha}\right). \tag{44}$$

Similarly, since $\mathbf{W}_{11}^{i+1}$ and G_{10}^{i+1} minimize J_1^{i+1} in (35), it readily follows that

$$\begin{aligned} J_1\left(\mathbf{W}_1^{i+1}\right) &= J_1^{i+1}\left(\mathbf{W}_{11}^{i+1}, G_{10}^{i+1}\right) \\ &\leq J_1^{i+1}\left(\alpha\mathbf{W}_{01}^i, \alpha\right) = J_1\left(\alpha\mathbf{W}_0^i\right). \end{aligned} \tag{45}$$

Using these inequalities and considering (42) and (43), it then follows that

$$\begin{aligned} J_1\left(\mathbf{W}_1^{i+1}\right) &\leq J_1\left(\alpha\mathbf{W}_0^i\right) = |\alpha|^2 J_0\left(\mathbf{W}_0^i\right) \\ &\leq |\alpha|^2 J_0\left(\frac{\mathbf{W}_1^i}{\alpha}\right) = J_1\left(\mathbf{W}_1^i\right). \end{aligned} \tag{46}$$

Similarly

$$\begin{aligned} J_0\left(\mathbf{W}_0^{i+1}\right) &\leq J_0\left(\frac{\mathbf{W}_1^{i+1}}{\alpha}\right) \\ &= \frac{J_1\left(\mathbf{W}_1^{i+1}\right)}{|\alpha|^2} \leq \frac{J_1\left(\alpha\mathbf{W}_0^i\right)}{|\alpha|^2} = J_0\left(\mathbf{W}_0^i\right). \end{aligned} \tag{47}$$

■

Secondly, from (38) the convergence of the DB-MWF procedure to the B-MWF solution in (25) can be proven, i.e.,

$$\boxed{\mathbf{W}_0^{\infty} = \mathbf{W}_0^m, \quad \mathbf{W}_1^{\infty} = \mathbf{W}_1^m} \tag{48}$$

Proof: Since the MWF cost functions in (34) and (35) are quadratic cost functions, the equality sign of the inequalities in (44) and (45) only holds if

$$\mathbf{W}_{00}^i = \frac{\mathbf{W}_{10}^i}{\alpha}, \quad G_{01}^i = \frac{1}{\alpha}, \quad \mathbf{W}_{11}^{i+1} = \alpha\mathbf{W}_{01}^i, \quad G_{10}^{i+1} = \alpha. \tag{49}$$

Hence, using (46) and (47), unless the condition in (49) is satisfied, the MWF cost functions are strictly decreasing, i.e.,

$$J_0\left(\mathbf{W}_0^{i+1}\right) < J_0\left(\mathbf{W}_0^i\right), \quad J_1\left(\mathbf{W}_1^{i+1}\right) < J_1\left(\mathbf{W}_1^i\right). \tag{50}$$

Since in the case of a single speech source, the B-MWF solution $\mathbf{W}_0^m$ and $\mathbf{W}_1^m$ in (25), minimizing the MWF cost functions $J_0(\mathbf{W})$ and $J_1(\mathbf{W})$, exactly satisfies (49), the DB-MWF procedure converges to this solution, i.e., $G_{10}^{\infty} = \alpha$ and $G_{01}^{\infty} = 1/\alpha$ in (37). ■

In the *general case* where $\mathbf{R}_x$ is not a rank-1 matrix, (38) does not hold, i.e., the MWF cost function does not necessarily decrease in each iteration, and the iterative DB-MWF procedure usually does not converge to the optimal filters $\mathbf{W}_0^m$ and $\mathbf{W}_1^m$ in (21), as these filters generally do not satisfy (37). However, extensive simulations show that, independent of the initial value for $\mathbf{W}_{11}^0$, the iterative DB-MWF procedure always converges to the same filters $\mathbf{W}_0^{\infty}$ and $\mathbf{W}_1^{\infty}$ and that the converged filters—not surprisingly—appear to provide the solution of the following constrained optimization problem: minimize the B-MWF cost function in (18), i.e.,

$$J(\mathbf{W}) = P - \mathbf{r}_x^H\mathbf{W} - \mathbf{W}^H\mathbf{r}_x + \mathbf{W}^H\mathbf{R}\mathbf{W} \tag{51}$$

subject to linear constraints as in (37), which can be rewritten as

$$\begin{bmatrix}\mathbf{I}_M & \mathbf{0}_M & \mathbf{0}_M & \mathbf{0}_M\end{bmatrix}\mathbf{W} = \rho_0\begin{bmatrix}\mathbf{0}_M & \mathbf{0}_M & \mathbf{I}_M & \mathbf{0}_M\end{bmatrix}\mathbf{W}, \quad \rho_0 \in \mathbb{C}, \tag{52}$$

$$\begin{bmatrix}\mathbf{0}_M & \mathbf{I}_M & \mathbf{0}_M & \mathbf{0}_M\end{bmatrix}\mathbf{W} = \rho_1\begin{bmatrix}\mathbf{0}_M & \mathbf{0}_M & \mathbf{0}_M & \mathbf{I}_M\end{bmatrix}\mathbf{W}, \quad \rho_1 \in \mathbb{C}. \tag{53}$$

This is stated here as an observation, as a formal proof is not available at this point. The solution of the above constrained optimization problem can be easily computed by reformulating the constraints in (52) and (53) and by solving the associated Lagrange dual problem (cf. Appendix B). Although the solution of the constrained optimization problem gives rise to higher cost functions, i.e.,

$$J_0\left(\mathbf{W}_0^{\infty}\right) \geq J_0\left(\mathbf{W}_0^m\right), \quad J_1\left(\mathbf{W}_1^{\infty}\right) \geq J_1\left(\mathbf{W}_1^m\right) \tag{54}$$

the experimental results in Section V show that the iterative DB-MWF procedure can still be used in practice and approaches the B-MWF performance in the general case where $\mathbf{R}_x$ is not a rank-1 matrix.

Note that throughout this section we have assumed iterations on the same block of data. To limit computational complexity in a real-time implementation, the iteration index i obviously will need to be replaced by a block (time) index, resulting in a time-recursive algorithm. However, if the signals can be assumed stationary for two or three blocks (cf. Section V-C), no performance degradation is expected. However, this paper does not elaborate on the time-recursive algorithm for the distributed binaural MWF procedure.

V. Experimental Results

In this section, experimental results are presented for a binaural hearing aid system with two microphones on each hearing aid. Section V-A describes the experimental setup and defines the typical parameter values and the performance measures used here. Section V-B compares the performance, i.e., SNR improvement and contralateral spatial directivity pattern, of the considered binaural noise reduction algorithms. In addition, Section V-C analyzes the effect of the number of iterations for the DB-MWF procedure, and in Sections V-D and V-E the influence of the FFT size and of VAD errors on the algorithms' performance is investigated.

A. Setup and Performance Measures

Two hearing aids with $M = 2$ omnidirectional microphones (Sonion 6378) each have been mounted on a CORTEX MK2 artificial head in a reverberant room. The distance between the microphones on each hearing aid is approximately 1 cm. By using acoustical curtains, the reverberation time of the room can be changed from $T_{60} \approx 140$ ms to $T_{60} \approx 500$ ms, where the latter condition is comparable to an average living room. Acoustic transfer functions between loudspeakers (Fostex 6301B) and all four microphones have been measured for both reverberation times, where the loudspeakers are placed at a distance of 1 m and at different angles from the head. The sampling frequency is equal to 20.48 kHz. Different speech and noise configurations have been considered (see Fig. 4):

- a speech source in front of the head ($\theta_x = 0°$) and several noise configurations θ_v : a single noise source at 60°, 90°, 120°, 180°, 270°, or 300°; two noise sources at $[-60°\ \ 60°]$, $[-120°\ \ 120°]$, or $[120°\ \ 210°]$; and four noise sources at $[60°\ \ 120°\ \ 180°\ \ 210°]$ (denoted as N4a in the figures) or $[60°\ \ 120°\ \ 180°\ \ 270°]$ (denoted as N4b in the figures);
- a speech source at the right side of the head ($\theta_x = 90°$) and a single noise source at $\theta_v = 180°$.

The speech source consists of four consecutive sentences from the HINT database [19], and the noise source is multi-talker babble noise (Auditec). For all configurations, the input broadband SNR is 0dB in the front microphone signal of the left hearing aid.

The FFT size used for frequency-domain processing is typically equal to $L = 128$, except in Section V-D the influence of the FFT size on the noise reduction performance is investigated. The MWF-based noise reduction procedures described in Sections III and IV are applied in each individual frequency bin.

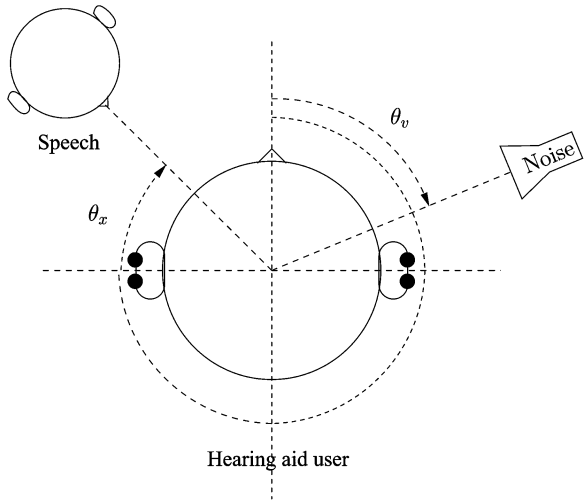

Fig. 4. Binaural hearing aid setup with speech and noise configuration.

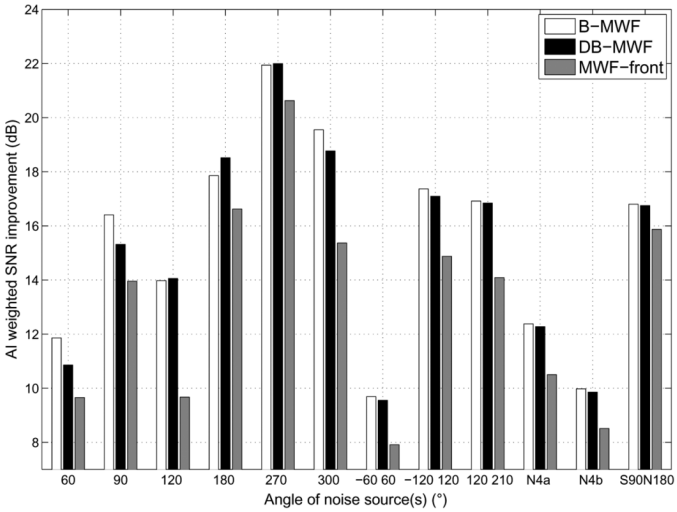

Fig. 5. ΔSNR_0 for B-MWF, MWF-front and DB-MWF ($K = 10$) for different configurations ($L = 128$, $T_{60} = 140$ ms).

Using a voice activity detector (VAD) on the complete signal (26 s), the noise correlation matrix $\mathbf{R}_v$ in each frequency bin is computed during noise-only periods, the correlation matrix $\mathbf{R}_y$ in each frequency bin is computed during speech-and-noise periods, and the speech correlation matrix in each frequency bin is estimated as $\mathbf{R}_x = \mathbf{R}_y - \mathbf{R}_v$. For most experiments, a perfect VAD has been used, except in Section V-E the influence of VAD errors on the algorithms' performance is investigated.

To assess the performance of the different algorithms, the broadband intelligibility weighted SNR improvement [20] between the output signal and the front microphone signal is computed, i.e., for the left and the right hearing aid

$$\Delta\text{SNR}_0 = \sum_l I(\omega_l)\left[\text{SNR}_{Z_0}(\omega_l) - \text{SNR}_{Y_{0,0}}(\omega_l)\right] \quad (55)$$

$$\Delta\text{SNR}_1 = \sum_l I(\omega_l)\left[\text{SNR}_{Z_1}(\omega_l) - \text{SNR}_{Y_{1,0}}(\omega_l)\right] \quad (56)$$

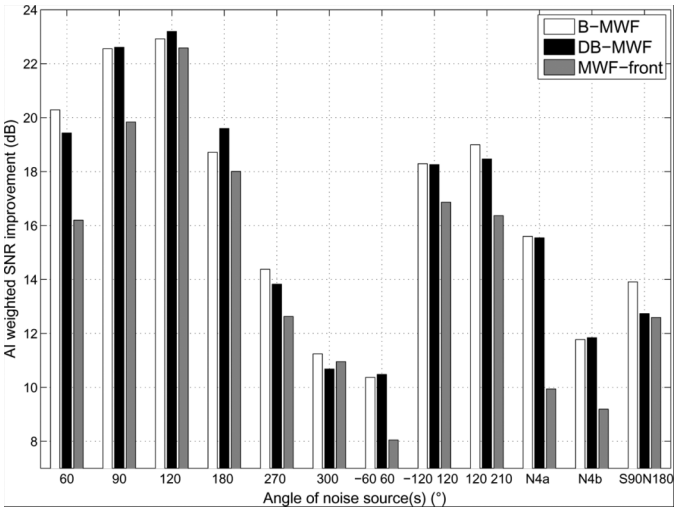

Fig. 6. ΔSNR_1 for B-MWF, MWF-front and DB-MWF ($K = 10$) for different configurations ($L = 128$, $T_{60} = 140$ ms).

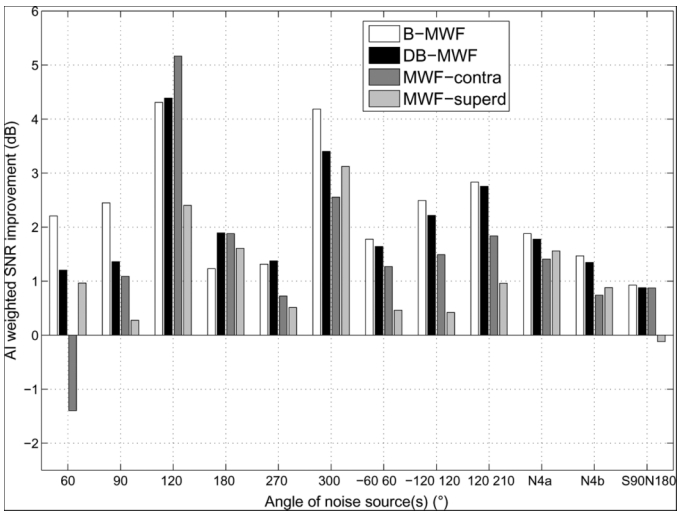

Fig. 7. ΔSNR_0 difference for B-MWF, MWF-contra, MWF-superd, and DB-MWF ($K = 10$) compared to MWF-front for different configurations ($L = 128$, $T_{60} = 140$ ms).

where $\text{SNR}_l(\omega_l)$ represents the SNR (in dB) in the lth frequency bin and $I(\omega_l)$ expresses the importance of the lth frequency bin for speech intelligibility [21].

For all MWF algorithms presented in Sections III and IV we have used $\mu = 5$. For MWF-superd discussed in Section IV-A, the superdirective beamformers $\mathbf{F}_{01}$ and $\mathbf{F}_{10}$ are computed as the (monaural) MWF solutions for the following configuration: a speech source in front of the head and noise sources arriving from all possible directions, i.e., every 30° in our setup; speech-weighted noise for both the speech and the noise sources; broadband input SNR equal to 0 dB in the front microphone signal. The fullband spatial directivity pattern of the resulting filter $\mathbf{F}_{01}$ is depicted in Fig. 9(d). Once computed, the same superdirective beamformers $\mathbf{F}_{01}$ and $\mathbf{F}_{10}$ are used for all considered speech and noise configurations, even the configuration where the speech source is located at 90°. For the iterative DB-MWF procedure discussed in Section IV-C, the number of iterations is

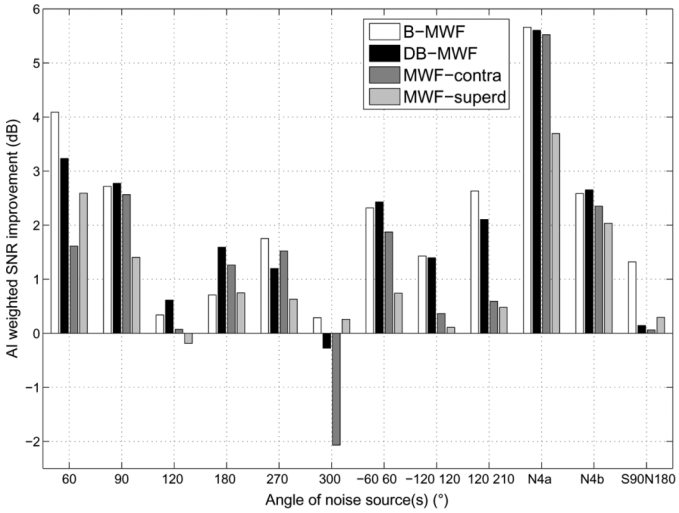

Fig. 8. ΔSNR_1 difference for B-MWF, MWF-contra, MWF-superd, and DB-MWF ($K = 10$) compared to MWF-front for different configurations ($L = 128$, $T_{60} = 140$ ms).

$K = 10$ (cf. Section V-C), and the filter $\mathbf{W}_{11}$ has been initialized to $\mathbf{W}_{11}^0 = [1 \quad 0 \quad \dots \quad 0]^T$, i.e., in the first iteration the front microphone signal of the right hearing aid is transmitted to the contralateral side.

B. SNR Improvement for Different Configurations and Reverberation Times

For all considered speech and noise configurations and for reverberation time $T_{60} = 140$ ms, Figs. 5 and 6 depict the SNR improvement at the left and the right hearing aid for the B-MWF, MWF-front, and the DB-MWF procedure. In order not to overload these figures, the performance of MWF-contra and MWF-superd has not been plotted on these figures, but the difference in SNR improvement compared to MWF-front has been plotted in Figs. 7 and 8. In general, for all algorithms the SNR improvement is larger when the speech source and the noise source(s) are spatially more separated, with the largest improvement occurring in the hearing aid where the input SNR is lower, e.g., for $\theta_v = 60°$ the SNR improvement is larger in the right hearing aid than in the left hearing aid.

From Figs. 5–8, the following observations can be made.

- The *B-MWF* (using four microphones) generally results in the largest SNR improvement of all algorithms, up to 4 dB better than MWF-front (using three microphones). Although B-MWF is theoretically optimal, for some configurations, e.g., $\theta_v = 120°$ and $\theta_v = 180°$, its performance is slightly lower than the performance of MWF-contra and the DB-MWF procedure, which might be due to estimation errors in the speech correlation matrices $\mathbf{R}_x$.
- The performance of *MWF-superd*, where a filtered combination of the contralateral microphone signals using a superdirective beamformer is transmitted, lies between the performance of MWF-front and B-MWF. The performance of MWF-superd is relatively better when the (signal-independent) spatial directivity pattern of the used superdirective beamformer approaches the optimal (signal-dependent) spatial directivity pattern of B-MWF,

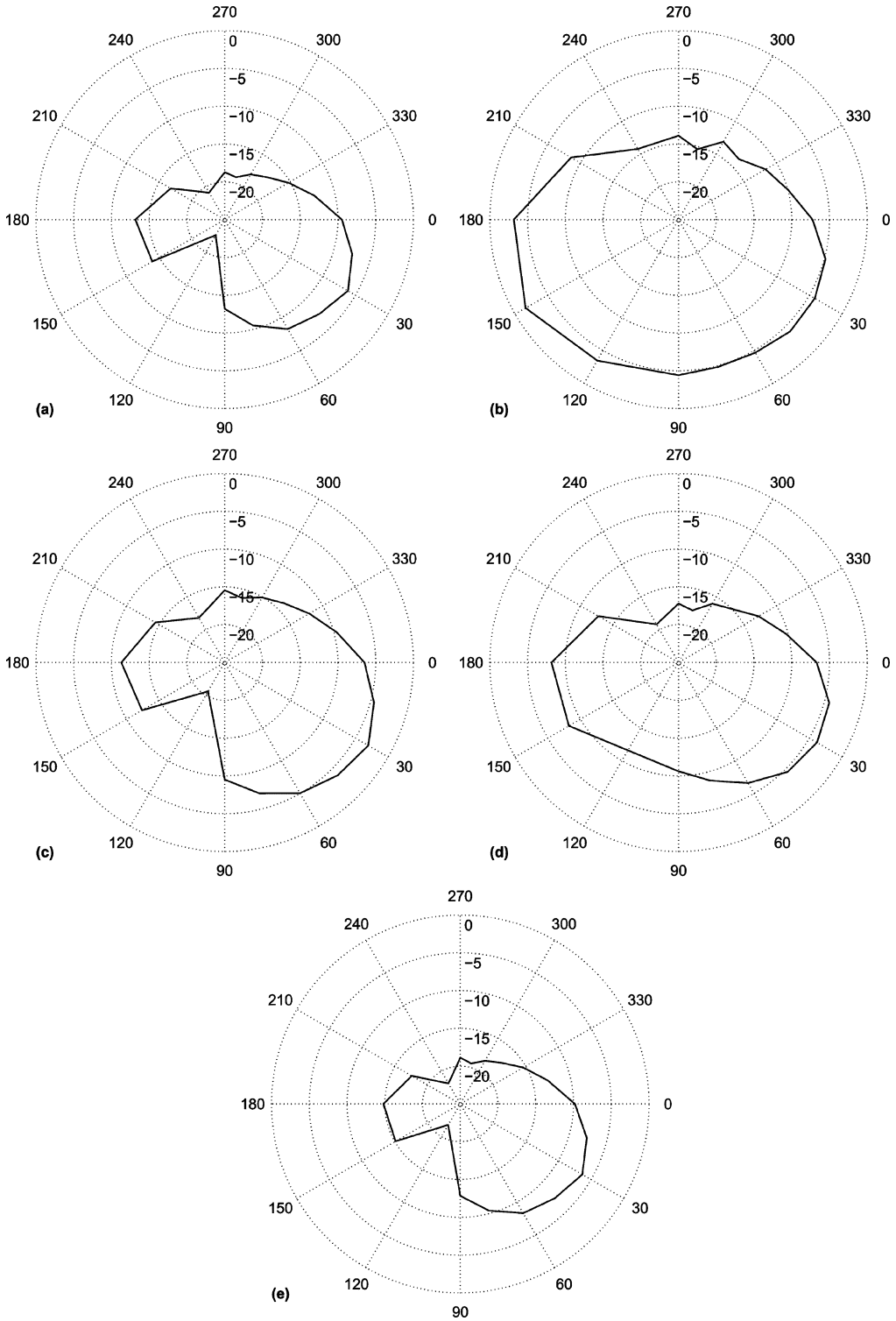

Fig. 9. Spatial directivity pattern of $\mathbf{F}_{01}$ with $\theta_v = [-120°, 120°]$ and $T_{60} = 140$ ms for (a) B-MWF, (b) MWF-front, (c) MWF-contra, (d) MWF-superd, (e) DB-MWF ($K = 10$).

which can e.g., be observed for ΔSNR_0 when $\theta_v = 300°$ or for ΔSNR_1 when $\theta_v = 60°$. However, in general, the performance of MWF-superd is worse than the performance of MWF-contra and DB-MWF. Obviously, a disadvantage of MWF-superd is the fact that the position of the speech source needs to be known for optimally designing the superdirective beamformer.

- The performance of *MWF-contra*, where the output of a monaural MWF on the contralateral microphone signals is transmitted, typically lies between the performance of MWF-front and B-MWF. However, for $\theta_v = 60°$ the SNR improvement in the left hearing aid is smaller than for MWF-front, which is likely due to the fact that using the monaural MWF $\mathbf{F}_{01}$ in (30), i.e., with two microphones, it

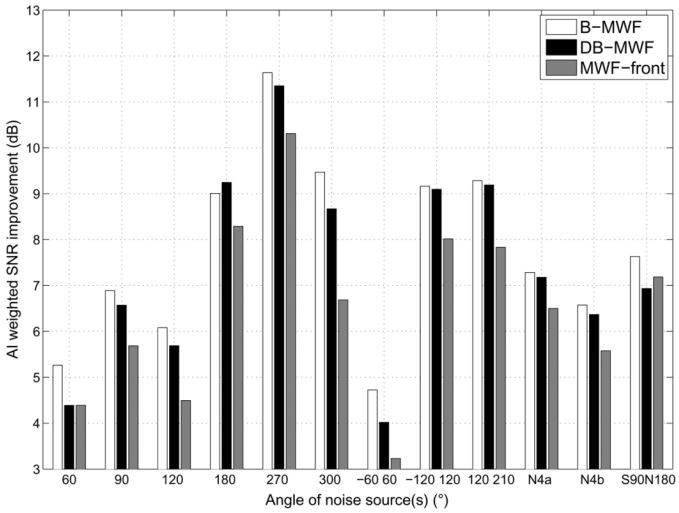

Fig. 10. ΔSNR_0 for B-MWF, MWF-front, and DB-MWF ($K = 10$) for different configurations ($L = 128$, $T_{60} = 500$ ms).

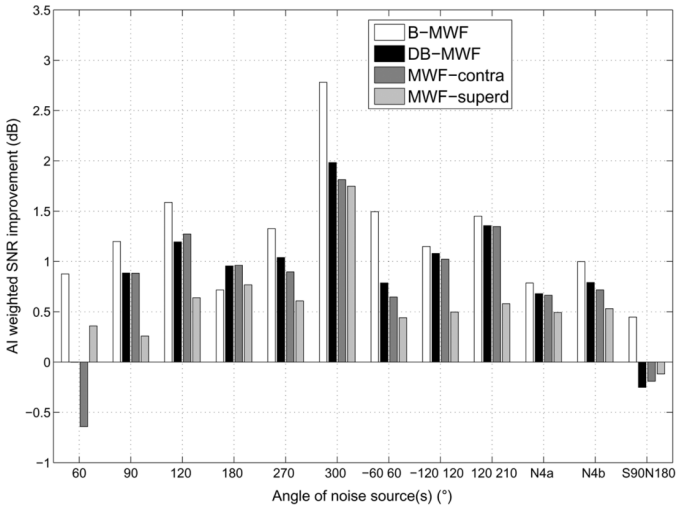

Fig. 12. ΔSNR_0

$_{60} = 500$ ms).

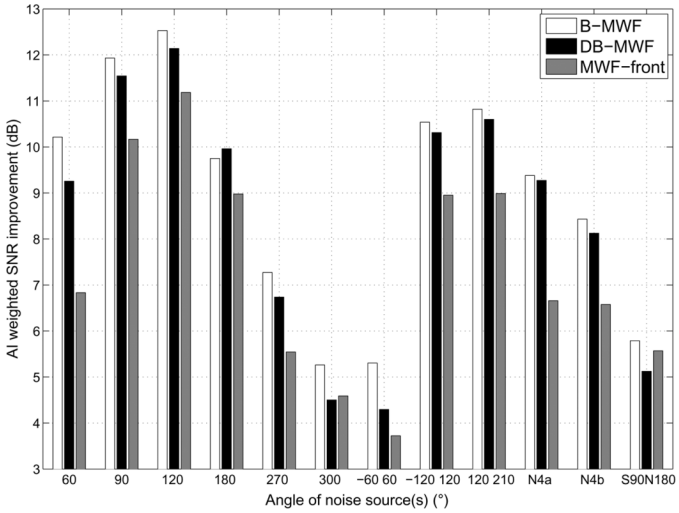

Fig. 11. ΔSNR_1 for B-MWF, MWF-front, and DB-MWF ($K = 10$) for different configurations ($L = 128$, $T_{60} = 500$ ms).

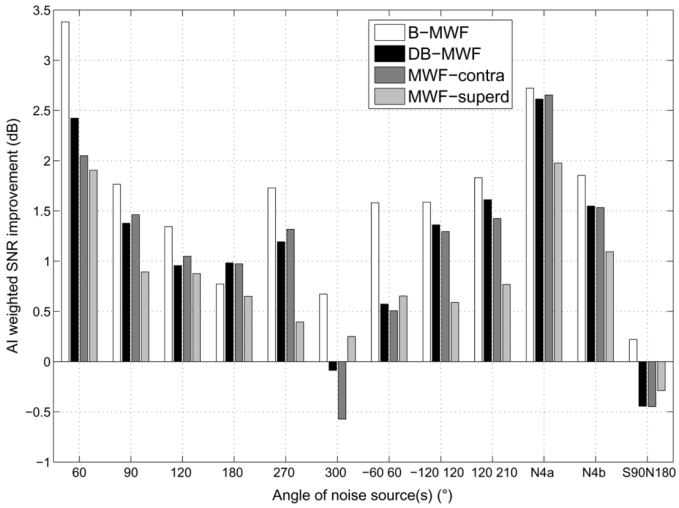

Fig. 13. ΔSNR_1 difference for B-MWF, MWF-contra, MWF-superd, and DB-MWF ($K = 10$) compared to MWF-front for different configurations ($L = 128$, $T_{60} = 500$ ms).

is not possible to approach the optimal spatial directivity pattern of the B-MWF well enough since the speech and the noise sources are located close to each other. A similar situation occurs for ΔSNR_1 when $\theta_v = 300°$.

- In general, the best performance of all presented reduced-bandwidth algorithms is achieved by the *DB-MWF* procedure, and compared to MWF-contra a substantial performance benefit is obtained, especially for $\theta_v = 60°$ and $\theta_v = 300°$ and when multiple noise sources are present.[1] Moreover, for most configurations the performance of the DB-MWF procedure approaches the performance of the B-MWF, even though in the simulations the speech correlation matrices $\mathbf{R}_x$ are not rank-1 matrices because of overlap between adjacent FFT frequency bins and by estimating the speech correlation matrices as $\mathbf{R}_x = \mathbf{R}_y - \mathbf{R}_v$.

For the configuration $\theta_v = [-120° \quad 120°]$ and for reverberation time $T_{60} = 140$ ms, Fig. 9 plots the fullband spatial directivity pattern of the filter $\mathbf{F}_{01}$, i.e., the pattern generated using the right microphone signals and transmitted to the left hearing aid. For the B-MWF [see Fig. 9(a)], it can be observed that a null is steered towards the direction of the noise sources, implying that optimally a signal with a high SNR should be transmitted to the contralateral side. Since this is not the case when transmitting the front microphone signal [see Fig. 9(b)], or when using the superdirective beamformer [see Fig. 9(d)], the SNR improvement in the left hearing aid substantially degrades for MWF-front and MWF-superd, as can be observed in Fig. 5. Since MWF-contra also suppresses the direction of the noise

[1]The configurations $\theta_v = 120°$ and $\theta_v = 270°$, where the performance of the DB-MWF procedure is slightly lower than the performance of MWF-contra, either in the left or the right hearing aid, need further investigation.

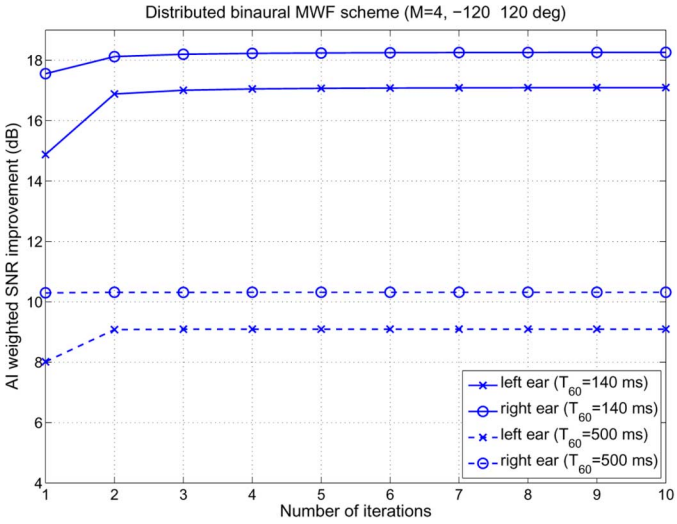

Fig. 14. SNR improvement at the left and the right hearing aid with $\theta_v = [-120°, 120°]$ for the iterative DB-MWF procedure as a function of the number of iterations ($L = 128$, $T_{60} = 140$ ms and 500 ms).

sources [see Fig. 9(c)], its performance is better than the performance of MWF-front and MWF-superd. The best performance is obtained by the DB-MWF procedure, as its spatial directivity pattern in Fig. 9(e) closely matches the spatial directivity pattern of the B-MWF in Fig. 9(a). Using these spatial directivity patterns, it is possible to some extent to explain the performance of the different algorithms for different noise configurations.

For the reverberation time $T_{60} = 500$ ms, Figs. 10–13 depict the SNR improvement in the left and the right hearing aid for all considered algorithms. Although the SNR improvements are smaller and hence also the differences between the algorithms are smaller, the same conclusions as for $T_{60} = 140$ ms hold, where in general the best performance of all presented reduced-bandwidth algorithms is achieved by the DB-MWF procedure and the performance of the DB-MWF procedure approaches quite well the performance of the B-MWF.

C. Influence of the Number of Iterations for DB-MWF

For the configuration $\theta_v = [-120° \; 120°]$ and for both reverberation times, Fig. 14 depicts the SNR improvement of the DB-MWF procedure in the left and the right hearing aid as a function of the number of iterations. This figure shows that already after two or three iterations the final performance is obtained, such that $K = 10$ certainly suffices for convergence of the iterative DB-MWF procedure. This has also been verified for other configurations.

D. Influence of the FFT Size

For the configuration $\theta_v = [-120° \quad 120°]$ and for reverberation time $T_{60} = 140$ ms, Fig. 15 depicts the SNR improvement in the left and the right hearing aid for different FFT sizes, ranging from 64 to 512. As can be expected, a better performance is obtained when using longer filter lengths. From this figure it can also be observed that for all FFT sizes the best performance of all presented reduced-bandwidth algorithms is

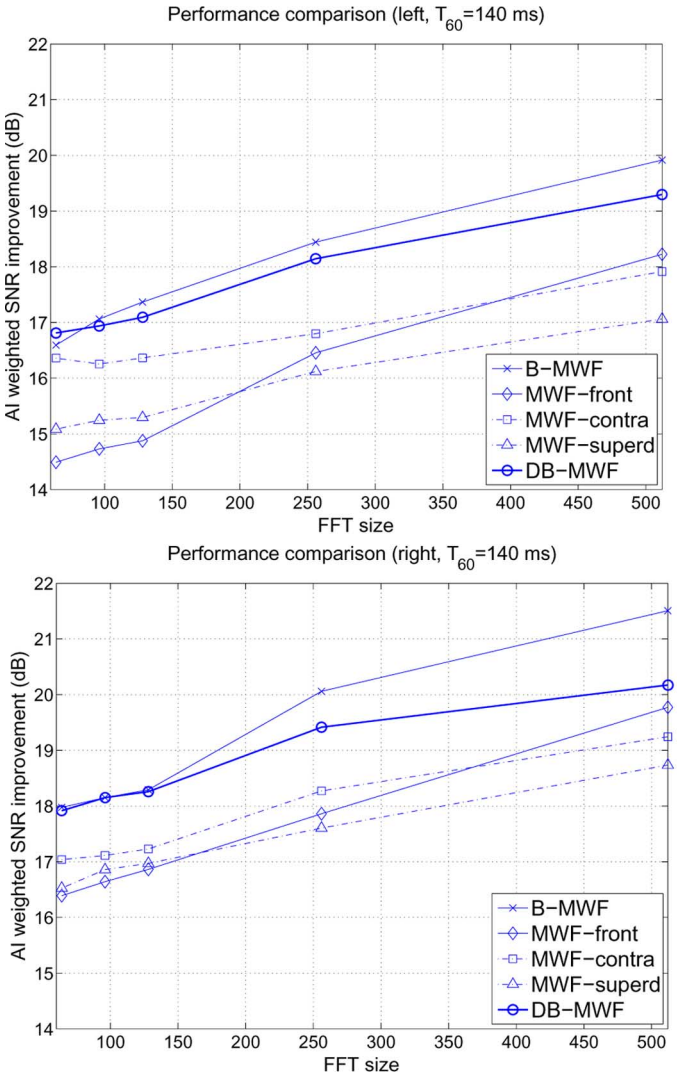

Fig. 15. SNR improvement at the left and the right hearing aid with $\theta_v = [-120°, 120°]$ for B-MWF, MWF-front, MWF-contra, MWF-superd, and DB-MWF ($K = 10$) as a function of the FFT size L ($T_{60} = 140$ ms).

achieved by the DB-MWF procedure, but that the difference between the B-MWF and the reduced-bandwidth algorithms (MWF-superd, MWF-contra, DB-MWF) increases as the FFT size increases, even to the point where the performance of MWF-superd and MWF-contra is smaller than the performance of MWF-front.

E. Influence of VAD Errors

In the previous sections, we have used a perfect VAD for computing the correlation matrices $\mathbf{R}_v$ and $\mathbf{R}_y$. In this section, we investigate the influence of VAD errors on the performance of the B-MWF, MWF-front, and DB-MWF procedure. We have systematically introduced two types of VAD errors: speech VAD errors, where speech-and-noise samples are detected as noise and δ_x represents the percentage of samples used to compute the noise correlation matrix $\mathbf{R}_v$ that are actually speech-and-noise samples, and noise VAD errors, where noise samples are detected as speech-and-noise and δ_v represents the percentage of

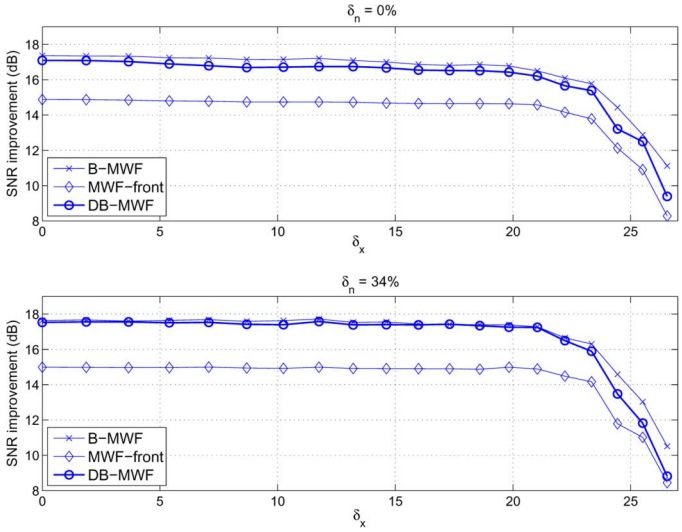

Fig. 16. SNR improvement at the left hearing aid with $\theta_v = [-120°, 120°]$ for B-MWF, MWF-front, and DB-MWF ($K = 10$) for different VAD errors ($L = 128$, $T_{60} = 140$ ms).

samples used to compute the correlation matrix $\mathbf{R}_y$ that are actually noise samples.[2]

For the configuration $\theta_v = [-120° \quad 120°]$ and for reverberation time $T_{60} = 140$ ms, Fig. 16 depicts the SNR improvement in the left hearing aid for different speech and noise VAD errors. This figure shows that the performance for all MWF algorithms degrades when δ_x (speech VAD errors) is larger than 20%, and that the performance is less sensitive to noise VAD errors. This corresponds to the conclusions obtained in [22]. Moreover, the performance of the DB-MWF procedure still approaches the performance of the B-MWF for all VAD errors, although the performance difference increases for larger δ_x.

[2]Throughout this paper, we have discussed batch versions of the MWF algorithms, where the correlation matrices $\mathbf{R}_v$ and $\mathbf{R}_y$ and the filter $\mathbf{W}$ are computed using the complete signal. Although introducing VAD errors in the batch versions gives an indication of the algorithms' sensitivity to VAD errors, it is important to realize that the sensitivity may be different for the adaptive (time-recursive) versions of the MWF algorithms, which are not discussed in this paper.

VI. Conclusion

The wireless link in a binaural hearing aid system typically does not allow to transmit all microphone signals between the hearing aids. In this paper, we have discussed several reduced-bandwidth MWF-based noise reduction algorithms, where only a filtered combination of the contralateral microphone signals is transmitted. Suboptimal schemes have been presented, either using the front contralateral microphone signal, using a fixed superdirective beamformer, or using the output of a monaural MWF on the contralateral microphone signals. In addition, an iterative distributed MWF procedure has been presented that converges to the binaural MWF solution in the case of a rank-1 speech correlation matrix and that approaches the binaural MWF solution if this rank-1 property is not satisfied. For a binaural hearing aid system with two microphones on each hearing aid, experimental results for several speech and noise configurations and for different reverberation times show that the best performance of all considered reduced-bandwidth algorithms is achieved by the DB-MWF procedure. Moreover, even though the speech correlation matrices in the simulations are not rank-1 matrices, the performance of the DB-MWF procedure approaches the performance of the binaural MWF. Further work will consist of transforming the iterative DB-MWF procedure to a time-recursive algorithm, lowering the computational complexity.

Appendix A

Proof for Contralateral MWF: If we define $\mathbf{R}_v$ using its submatrices as

$$\mathbf{R}_v = \begin{bmatrix} \mathbf{R}_v^{00} & \mathbf{R}_v^{01} \\ \mathbf{R}_v^{10} & \mathbf{R}_v^{11} \end{bmatrix} \tag{57}$$

then the inverse of this matrix is equal to (58), as shown at the bottom of the page, with $\mathbf{S}_{v0} = \mathbf{R}_v^{11} - \mathbf{R}_v^{10}(\mathbf{R}_v^{00})^{-1}\mathbf{R}_v^{01}$ and $\mathbf{S}_{v1} = \mathbf{R}_v^{00} - \mathbf{R}_v^{01}(\mathbf{R}_v^{11})^{-1}\mathbf{R}_v^{10}$.

In the case of a *single speech source*, the filters $\mathbf{W}_{01}^m$ and $\mathbf{W}_{10}^m$ can be written, using (25) and (58), as shown n (59)–(60) at the bottom of the next page, and the filters $\mathbf{F}_{01}$ and $\mathbf{F}_{10}$ in

$$\mathbf{R}_v^{-1} = \begin{bmatrix} (\mathbf{R}_v^{00})^{-1} + \left(\mathbf{R}_v^{00}\right)^{-1}\mathbf{R}_v^{01}\mathbf{S}_{v0}^{-1}\mathbf{R}_v^{10}\left(\mathbf{R}_v^{00}\right)^{-1} & -\left(\mathbf{R}_v^{00}\right)^{-1}\mathbf{R}_v^{01}\mathbf{S}_{v0}^{-1} \\ -\left(\mathbf{R}_v^{11}\right)^{-1}\mathbf{R}_v^{10}\mathbf{S}_{v1}^{-1} & \left(\mathbf{R}_v^{11}\right)^{-1} + \left(\mathbf{R}_v^{11}\right)^{-1}\mathbf{R}_v^{10}\mathbf{S}_{v1}^{-1}\mathbf{R}_v^{01}\left(\mathbf{R}_v^{11}\right)^{-1} \end{bmatrix} \tag{58}$$

$$\mathbf{W}_{01}^m = \mathbf{Q}_1 \frac{\mathbf{R}_v^{-1}\mathbf{A}}{\mathbf{A}^H\mathbf{R}_v^{-1}\mathbf{A} + \frac{\mu}{P_s}} A_{0,0}^* = \frac{-\left(\mathbf{R}_v^{11}\right)^{-1}\mathbf{R}_v^{10}\mathbf{S}_{v1}^{-1}\mathbf{A}_0 + \left[\left(\mathbf{R}_v^{11}\right)^{-1} + \left(\mathbf{R}_v^{11}\right)^{-1}\mathbf{R}_v^{10}\mathbf{S}_{v1}^{-1}\mathbf{R}_v^{01}\left(\mathbf{R}_v^{11}\right)^{-1}\right]\mathbf{A}_1}{\mathbf{A}^H\mathbf{R}_v^{-1}\mathbf{A} + \frac{\mu}{P_s}} A_{0,0}^* \tag{59}$$

$$\mathbf{W}_{10}^m = \mathbf{Q}_0 \frac{\mathbf{R}_v^{-1}\mathbf{A}}{\mathbf{A}^H\mathbf{R}_v^{-1}\mathbf{A} + \frac{\mu}{P_s}} A_{1,0}^* = \frac{\left[(\mathbf{R}_v^{00})^{-1} + (\mathbf{R}_v^{00})^{-1}\mathbf{R}_v^{01}\mathbf{S}_{v0}^{-1}\mathbf{R}_v^{10}(\mathbf{R}_v^{00})^{-1}\right]\mathbf{A}_0 - (\mathbf{R}_v^{00})^{-1}\mathbf{R}_v^{01}\mathbf{S}_{v0}^{-1}\mathbf{A}_1}{\mathbf{A}^H\mathbf{R}_v^{-1}\mathbf{A} + \frac{\mu}{P_s}} A_{1,0}^* \tag{60}$$

(32) and (33) are equal to

$$\mathbf{F}_{01} = \frac{(\mathbf{R}_v^{11})^{-1}\mathbf{A}_1}{\mathbf{A}_1^H(\mathbf{R}_v^{11})^{-1}\mathbf{A}_1 + \frac{\mu}{P_s}} A_{1,0}^*$$
$$\mathbf{F}_{10} = \frac{(\mathbf{R}_v^{00})^{-1}\mathbf{A}_0}{\mathbf{A}_0^H(\mathbf{R}_v^{00})^{-1}\mathbf{A}_0 + \frac{\mu}{P_s}} A_{0,0}^*. \quad (61)$$

Generally, $\mathbf{F}_{01}$ is not parallel to $\mathbf{W}_{01}^m$ and $\mathbf{F}_{10}$ is not parallel to $\mathbf{W}_{10}^m$. However, when the noise components between the left and the right hearing aid are uncorrelated, i.e., $\mathbf{R}_v^{01} = \mathbf{R}_v^{10} = \mathbf{0}$, the filters $\mathbf{W}_{01}^m$ and $\mathbf{W}_{10}^m$ in (59) and (60) reduce to

$$\mathbf{W}_{01}^m = \frac{(\mathbf{R}_v^{11})^{-1}\mathbf{A}_1}{\mathbf{A}^H\mathbf{R}_v^{-1}\mathbf{A} + \frac{\mu}{P_s}} A_{0,0}^*$$
$$\mathbf{W}_{10}^m = \frac{(\mathbf{R}_v^{00})^{-1}\mathbf{A}_0}{\mathbf{A}^H\mathbf{R}_v^{-1}\mathbf{A} + \frac{\mu}{P_s}} A_{1,0}^* \quad (62)$$

such that $\mathbf{F}_{01}$ is parallel to $\mathbf{W}_{01}^m$ and $\mathbf{F}_{10}$ is parallel to $\mathbf{W}_{10}^m$.

In the *general case* where $\mathbf{R}_x$ is not a rank-1 matrix, the filters $\mathbf{W}_{01}^m$ and $\mathbf{W}_{10}^m$ can be written, using (21), as shown in (63)–(64) at the bottom of the page, with $\mathbf{R}_t = \mathbf{R}_x + \mu\mathbf{R}_v$. The filters $\mathbf{F}_{01}$ and $\mathbf{F}_{10}$ in (32) and (33) are equal to

$$\mathbf{F}_{01} = \left(\mathbf{R}_t^{11}\right)^{-1}\mathbf{Q}_1\mathbf{r}_{x1}, \quad \mathbf{F}_{10} = \left(\mathbf{R}_t^{00}\right)^{-1}\mathbf{Q}_0\mathbf{r}_{x0}. \quad (65)$$

In general, no relationship exists between $\mathbf{r}_{x0}$ and $\mathbf{r}_{x1}$, such that $\mathbf{F}_{01}$ is not parallel to $\mathbf{W}_{01}^m$ and $\mathbf{F}_{10}$ is not parallel to $\mathbf{W}_{10}^m$. This is not even the case when the speech and the noise components between the left and the right hearing aid are uncorrelated, i.e., $\mathbf{R}_t^{01} = \mathbf{R}_t^{10} = \mathbf{0}$, and the filters $\mathbf{W}_{01}^m$ and $\mathbf{W}_{10}^m$ in (63) and (64) reduce to

$$\mathbf{W}_{01}^m = \left(\mathbf{R}_t^{11}\right)^{-1}\mathbf{Q}_1\mathbf{r}_{x0}, \quad \mathbf{W}_{10}^m = \left(\mathbf{R}_t^{00}\right)^{-1}\mathbf{Q}_0\mathbf{r}_{x1}. \quad (66)$$

APPENDIX B

CONSTRAINED OPTIMIZATION PROBLEM FOR THE GENERAL CASE:

In order to solve the constrained optimization problem

$$\min_{\mathbf{W}} J(\mathbf{W}) = P - \mathbf{r}_x^H\mathbf{W} - \mathbf{W}^H\mathbf{r}_x + \mathbf{W}^H\mathbf{R}\mathbf{W} \quad (67)$$

$$[\mathbf{I}_M \ \mathbf{0}_M \ \mathbf{0}_M \ \mathbf{0}_M]\mathbf{W} = \rho_0[\mathbf{0}_M \ \mathbf{0}_M \ \mathbf{I}_M \ \mathbf{0}_M]\mathbf{W}, \quad \rho_0 \in \mathbb{C} \quad (68)$$

$$[\mathbf{0}_M \ \mathbf{I}_M \ \mathbf{0}_M \ \mathbf{0}_M]\mathbf{W} = \rho_1[\mathbf{0}_M \ \mathbf{0}_M \ \mathbf{0}_M \ \mathbf{I}_M]\mathbf{W}, \quad \rho_1 \in \mathbb{C} \quad (69)$$

we first reformulate the constraints by eliminating the (unknown) variables ρ_0 and ρ_1. We then consider the associated Lagrange dual problem, which is known to be a convex problem and hence can be easily optimized.

The constraints in (68) and (69) correspond to $\mathbf{W}_{00}$ being parallel to $\mathbf{W}_{10}$ and $\mathbf{W}_{01}$ being parallel to $\mathbf{W}_{11}$, i.e.,

$$\rho_0 = \frac{W_{00,0}}{W_{10,0}} = \frac{W_{00,m}}{W_{10,m}}, \quad \rho_1 = \frac{W_{01,0}}{W_{11,0}} = \frac{W_{01,m}}{W_{11,m}}, \quad m = 1 \ldots M-1. \quad (70)$$

These expressions can be reformulated as $2(M-1)$ quadratic constraints by eliminating ρ_0 and ρ_1, i.e.,

$$W_{00,0}W_{10,m} - W_{10,0}W_{00,m} = 0,$$
$$W_{01,0}W_{11,m} - W_{11,0}W_{01,m} = 0, \quad m = 1 \ldots M-1, \quad (71)$$

which can be written as

$$\mathbf{W}^T\mathbf{C}_{0m}\mathbf{W} = 0, \quad \mathbf{W}^T\mathbf{C}_{1m}\mathbf{W} = 0, \quad m = 1 \ldots M-1 \quad (72)$$

with the $4M \times 4M$-dimensional symmetric matrices $\mathbf{C}_{0m}$ and $\mathbf{C}_{1m}$ and the $M \times M$-dimensional anti-symmetric matrix $\mathbf{T}_m$ defined as

$$\mathbf{C}_{0m} = \left[\begin{array}{cc|cc} & & \mathbf{T}_m & \mathbf{0}_M \\ & \mathbf{0}_{2M} & \mathbf{0}_M & \mathbf{0}_M \\ \hline -\mathbf{T}_m & \mathbf{0}_M & & \\ \mathbf{0}_M & \mathbf{0}_M & \multicolumn{2}{c}{\mathbf{0}_{2M}} \end{array}\right]$$
$$\mathbf{C}_{1m} = \left[\begin{array}{cc|cc} & & \mathbf{0}_M & \mathbf{0}_M \\ & \mathbf{0}_{2M} & \mathbf{0}_M & \mathbf{T}_m \\ \hline \mathbf{0}_M & \mathbf{0}_M & & \\ \mathbf{0}_M & -\mathbf{T}_M & \multicolumn{2}{c}{\mathbf{0}_{2M}} \end{array}\right]$$
$$\mathbf{T}_m = \left[\begin{array}{c|ccc} 0 & \ldots & 1 & \ldots \\ \hline \vdots & & & \\ -1 & & \mathbf{0}_{M-1} & \\ \vdots & & & \end{array}\right]. \quad (73)$$

The matrices $\mathbf{C}_{0m}$ and $\mathbf{C}_{1m}$ are indefinite, since they have two eigenvalues equal to 1, two eigenvalues equal to -1, and $4(M-1)$ eigenvalues equal to 0. Since the appearance of the transpose $\mathbf{W}^T$ instead of the Hermitian transpose $\mathbf{W}^H$ in the constraints (72) hampers further operations, such as gradient calculation, we reformulate the cost function (67) and the constraints (72) using real-valued variables. We decompose $\mathbf{W}$, $\mathbf{r}_x$ and $\mathbf{R}$ into their real and imaginary parts, i.e.,

$$\mathbf{W} = \mathbf{W}_R + j\mathbf{W}_I, \quad \mathbf{r}_x = \mathbf{r}_{xR} + j\mathbf{r}_{xI}, \quad \mathbf{R} = \mathbf{R}_R + j\mathbf{R}_I. \quad (74)$$

$$\mathbf{W}_{01}^m = \mathbf{Q}_1\mathbf{R}_t^{-1}\mathbf{r}_{x0} = -\left(\mathbf{R}_t^{11}\right)^{-1}\mathbf{R}_t^{10}\mathbf{S}_1^{-1}\mathbf{Q}_0\mathbf{r}_{x0} + \left[\left(\mathbf{R}_t^{11}\right)^{-1} + \left(\mathbf{R}_t^{11}\right)^{-1}\mathbf{R}_t^{10}\mathbf{S}_1^{-1}\mathbf{R}_t^{01}\left(\mathbf{R}_t^{11}\right)^{-1}\right]\mathbf{Q}_1\mathbf{r}_{x0} \quad (63)$$

$$\mathbf{W}_{10}^m = \mathbf{Q}_0\mathbf{R}_t^{-1}\mathbf{r}_{x1} = \left[\left(\mathbf{R}_t^{00}\right)^{-1} + \left(\mathbf{R}_t^{00}\right)^{-1}\mathbf{R}_t^{01}\mathbf{S}_0^{-1}\mathbf{R}_t^{10}\left(\mathbf{R}_t^{00}\right)^{-1}\right]\mathbf{Q}_0\mathbf{r}_{x1} - \left(\mathbf{R}_t^{00}\right)^{-1}\mathbf{R}_t^{01}\mathbf{S}_0^{-1}\mathbf{Q}_1\mathbf{r}_{x1} \quad (64)$$

It can be easily shown that the optimization problem in (67) can be rewritten as

$$\boxed{\min_{\tilde{\mathbf{W}}} J(\tilde{\mathbf{W}}) = P - 2\tilde{\mathbf{r}}_x^T\tilde{\mathbf{W}} + \tilde{\mathbf{W}}^T\tilde{\mathbf{R}}\tilde{\mathbf{W}}} \tag{75}$$

with the real-valued variables $\tilde{\mathbf{W}}$, $\tilde{\mathbf{r}}_x$ and $\tilde{\mathbf{R}}$ defined as

$$\tilde{\mathbf{W}} = \begin{bmatrix} \mathbf{W}_R \\ \mathbf{W}_I \end{bmatrix}, \quad \tilde{\mathbf{r}}_x = \begin{bmatrix} \mathbf{r}_{xR} \\ \mathbf{r}_{xI} \end{bmatrix}, \quad \tilde{\mathbf{R}} = \begin{bmatrix} \mathbf{R}_R & \mathbf{R}_I \\ -\mathbf{R}_I & \mathbf{R}_R \end{bmatrix} \tag{76}$$

and that the constraints in (72) can be rewritten as

$$\begin{aligned} \tilde{\mathbf{W}}^T\tilde{\mathbf{C}}_{0m,R}\tilde{\mathbf{W}} = 0, \quad \tilde{\mathbf{W}}^T\tilde{\mathbf{C}}_{0m,I}\tilde{\mathbf{W}} = 0 \\ \tilde{\mathbf{W}}^T\tilde{\mathbf{C}}_{1m,R}\tilde{\mathbf{W}} = 0, \quad \tilde{\mathbf{W}}^T\tilde{\mathbf{C}}_{1m,I}\tilde{\mathbf{W}} = 0 \\ m = 1 \ldots M-1 \end{aligned} \tag{77}$$

with

$$\begin{aligned} \tilde{\mathbf{C}}_{km,R} = \begin{bmatrix} \mathbf{C}_{km} & \mathbf{0}_{4M} \\ \mathbf{0}_{4M} & -\mathbf{C}_{km} \end{bmatrix} \quad \tilde{\mathbf{C}}_{km,I} = \begin{bmatrix} \mathbf{0}_{4M} & \mathbf{C}_{km} \\ \mathbf{C}_{km} & \mathbf{0}_{4M} \end{bmatrix} \\ k = 0, 1, \quad m = 1 \ldots M-1. \end{aligned} \tag{78}$$

Note that $\tilde{\mathbf{R}}$, $\tilde{\mathbf{C}}_{km,R}$, and $\tilde{\mathbf{C}}_{km,I}$ are symmetric matrices. For convenience, we will rewrite the $N = 4(M-1)$ constraints in (77) as

$$\boxed{\tilde{\mathbf{W}}^T\tilde{\mathbf{J}}_n\tilde{\mathbf{W}} = 0, \quad n = 1 \ldots N}. \tag{79}$$

To solve the constrained optimization problem in (75) and (79), we consider the associated (unconstrained) Lagrange dual problem[3] [23]. The Lagrange dual problem is defined as the maximization of the Lagrange dual function $g(\lambda)$, which is the infimum of the Lagrangian $L(\tilde{\mathbf{W}}, \boldsymbol{\lambda})$, i.e.,

$$\boxed{\max_{\boldsymbol{\lambda}} g(\boldsymbol{\lambda}) = \max_{\boldsymbol{\lambda}} \left\{ \inf_{\tilde{\mathbf{W}}} L(\tilde{\mathbf{W}}, \boldsymbol{\lambda}) \right\}} \tag{80}$$

where the Lagrangian $L(\tilde{\mathbf{W}}, \boldsymbol{\lambda})$ is defined as

$$\begin{aligned} L(\tilde{\mathbf{W}}, \boldsymbol{\lambda}) &= J(\tilde{\mathbf{W}}) + \sum_{n=1}^{N} \lambda_n \tilde{\mathbf{W}}^T\tilde{\mathbf{J}}_n\tilde{\mathbf{W}} \\ &= P - 2\tilde{\mathbf{r}}_x^T\tilde{\mathbf{W}} + \tilde{\mathbf{W}}^T \left[\tilde{\mathbf{R}} + \sum_{n=1}^{N} \lambda_n \tilde{\mathbf{J}}_n \right] \tilde{\mathbf{W}}, \end{aligned} \tag{81}$$

with $\boldsymbol{\lambda}$ the Lagrange multipliers. The Lagrange dual problem (80) is a convex optimization problem in the Lagrange multipliers, for which the solution -in the case of strong duality- corresponds to the solution of the associated constrained optimization problem [23]. When $\tilde{\mathbf{R}} + \sum_{n=1}^{N} \lambda_n \tilde{\mathbf{J}}_n$ is a positive definite matrix, the Lagrange dual function is equal to

$$\boxed{g(\boldsymbol{\lambda}) = P - \tilde{\mathbf{r}}_x^T \left[\tilde{\mathbf{R}} + \textstyle\sum_{n=1}^{N} \lambda_n \tilde{\mathbf{J}}_n \right]^{-1} \tilde{\mathbf{r}}_x} \tag{82}$$

[3]Note that the constrained optimization problem appears to be non-convex, since the matrices $\bar{\mathbf{J}}_n$ in (79) are not positive definite.

corresponding to the filter

$$\tilde{\mathbf{W}} = \left[\tilde{\mathbf{R}} + \sum_{n=1}^{N} \lambda_n \tilde{\mathbf{J}}_n \right]^{-1} \tilde{\mathbf{r}}_x. \tag{83}$$

When this matrix is not positive definite, $g(\boldsymbol{\lambda}) = -\infty$. The Lagrange multipliers for which $g(\boldsymbol{\lambda}) > -\infty$ are called dual feasible. Although no closed-form solution exists for the Lagrange multipliers maximizing $g(\boldsymbol{\lambda})$ in (82), this concave function can be easily maximized using an iterative, e.g., quasi-Newton, method [24]. In order to improve the numerical robustness and convergence speed, both the gradient and the Hessian, i.e.,

$$\frac{\partial g(\boldsymbol{\lambda})}{\partial \lambda_n} = \tilde{\mathbf{r}}_x^T \left[\tilde{\mathbf{R}} + \sum_{n=1}^{N} \lambda_n \tilde{\mathbf{J}}_n \right]^{-1} \tilde{\mathbf{J}}_n \left[\tilde{\mathbf{R}} + \sum_{n=1}^{N} \lambda_n \tilde{\mathbf{J}}_n \right]^{-1} \tilde{\mathbf{r}}_x \tag{84}$$

$$\begin{aligned} \frac{\partial^2 g(\boldsymbol{\lambda})}{\partial \lambda_m \lambda_n} = &- 2\tilde{\mathbf{r}}_x^T \left[\tilde{\mathbf{R}} + \sum_{n=1}^{N} \lambda_n \tilde{\mathbf{J}}_n \right]^{-1} \\ &\times \tilde{\mathbf{J}}_m \left[\tilde{\mathbf{R}} + \sum_{n=1}^{N} \lambda_n \tilde{\mathbf{J}}_n \right]^{-1} \tilde{\mathbf{J}}_n \left[\tilde{\mathbf{R}} + \sum_{n=1}^{N} \lambda_n \tilde{\mathbf{J}}_n \right]^{-1} \tilde{\mathbf{r}}_x \end{aligned} \tag{85}$$

can be supplied analytically. Since $\tilde{\mathbf{R}}$ is a positive definite matrix, $\boldsymbol{\lambda} = \mathbf{0}$ always is dual feasible and can be used as an initial value.

REFERENCES

[1] B. Kollmeier, J. Peissig, and V. Hohmann, "Real-time multiband dynamic compression and noise reduction for binaural hearing aids," *J. Rehab. Res. Dev.*, vol. 30, no. 1, pp. 82–94, 1993.

[2] J. Desloge, W. Rabinowitz, and P. Zurek, "Microphone-array hearing aids with binaural output-Part I: Fixed-processing systems," *IEEE Trans. Speech Audio Process.*, vol. 5, no. 6, pp. 529–542, Nov. 1997.

[3] D. Welker, J. Greenberg, J. Desloge, and P. Zurek, "Microphone-array hearing aids with binaural output-Part II: A two-microphone adaptive system," *IEEE Trans. Speech Audio Process.*, vol. 5, no. 6, pp. 543–551, Nov. 1997.

[4] I. Merks, M. Boone, and A. Berkhout, "Design of a broadside array for a binaural hearing aid," in *Proc. IEEE Workshop Applicat, Signal Process. to Audio and Acoust. (WASPAA)*, New Paltz, NY, Oct. 1997, pp. 1–4.

[5] V. Hamacher, "Comparison of advanced monaural and binaural noise reduction algorithms for hearing aids," in *Proc. IEEE Int. Conf. Acoustics, Speech, and Signal Processing (ICASSP)*, Orlando, FL, May 2002, pp. 4008–4011.

[6] R. Nishimura, Y. Suzuki, and F. Asano, "A new adaptive binaural microphone array system using a weighted least squares algorithm," in *Proc. IEEE Int. Conf. Acoust., Speech, Signal Process. (ICASSP)*, Orlando, FL, May 2002, pp. 1925–1928.

[7] T. Wittkop and V. Hohmann, "Strategy-selective noise reduction for binaural digital hearing aids," *Speech Commun.*, vol. 39, no. 1–2, pp. 111–138, Jan. 2003.

[8] M. Lockwood, D. Jones, R. Bilger, C. Lansing, W. O'Brien, B. Wheeler, and A. Feng, "Performance of time- and frequency-domain binaural beamformers based on recorded signals from real rooms," *J. Acoust. Soc. Amer.*, vol. 115, no. 1, pp. 379–391, Jan. 2004.

[9] T. Lotter and P. Vary, "Dual-channel speech enhancement by superdirective beamforming," *EURASIP J. Appl. Signal Process.*, vol. 2006, 2006, article ID 63297.

[10] O. Roy and M. Vetterli, "Rate-constrained beamforming for collaborating hearing aids," in *Proc. Int. Symp. Inf. Theory (ISIT)*, Seattle, WA, Jul. 2006, pp. 2809–2813.

[11] T. Klasen, T. Van den Bogaert, M. Moonen, and J. Wouters, "Binaural noise reduction algorithms for hearing aids that preserve interaural time delay cues," *IEEE Trans. Signal Process.*, vol. 55, no. 4, pp. 1579–1585, Apr. 2007.

[12] S. Doclo, R. Dong, T. J. Klasen, J. Wouters, S. Haykin, and M. Moonen, "Extension of the multi-channel Wiener filter with localisation cues for noise reduction in binaural hearing aids," in *Proc. Int. Workshop Acoust. Echo and Noise Control (IWAENC)*, Eindhoven, The Netherlands, Sep. 2005, pp. 221–224.
[13] S. Doclo, T. J. Klasen, T. Van den Bogaert, J. Wouters, and M. Moonen, "Theoretical analysis of binaural cue preservation using multi-channel Wiener filtering and interaural transfer functions," in *Proc. Int. Workshop Acoust. Echo and Noise Control (IWAENC)*, Paris, France, Sep. 2006.
[14] T. Van den Bogaert, S. Doclo, M. Moonen, and J. Wouters, "Binaural cue preservation for hearing aids using an interaural transfer function multichannel Wiener filter," in *Proc. IEEE Int. Conf. Acoust., Speech, Signal Process. (ICASSP)*, Honolulu, HI, Apr. 2007, pp. 565–568.
[15] "E2e Wireless Technical Overview." [Online]. Available: http://mysiemens.siemens-hearing.com/admin/documents/10053817e2eWirelessOverview.pdf
[16] A. Boothroyd, K. Fitz, J. Kindred, S. Kochkin, H. Levitt, B. Moore, and J. Yantz, "Hearing aids and wireless technology," *Hearing Rev.*, vol. 14, no. 6, pp. 44–48, Jun. 2007.
[17] S. Doclo and M. Moonen, "GSVD-based optimal filtering for single and multimicrophone speech enhancement," *IEEE Trans. Signal Process.*, vol. 50, pp. 2230–2244, Sep. 2002.
[18] S. Doclo, A. Spriet, J. Wouters, and M. Moonen, "Frequency-domain criterion for speech distortion weighted multichannel Wiener filter for robust noise reduction," *Speech Commun.*, vol. 49, no. 7–8, pp. 636–656, Jul.–Aug. 2007.
[19] M. Nilsson, S. D. Soli, and A. Sullivan, "Development of the hearing in noise test for the measurement of speech reception thresholds in quiet and in noise," *J. Acoust. Soc. Amer.*, vol. 95, no. 2, pp. 1085–1099, Feb. 1994.
[20] J. E. Greenberg, P. M. Peterson, and P. M. Zurek, "Intelligibility-weighted measures of speech-to-interference ratio and speech system performance," *J. Acoust. Soc. Amer.*, vol. 94, no. 5, pp. 3009–3010, Nov. 1993.
[21] *American National Standard Methods for Calculation of the Speech Intelligibility Index*, ANSI S3.5–1997, Acoust. Soc. Amer., 1997.
[22] A. Spriet, M. Moonen, and J. Wouters, "The impact of speech detection errors on the noise reduction performance of multi-channel Wiener filtering and generalized sidelobe cancellation," *Signal Process.*, vol. 85, no. 6, pp. 1073–1088, Jun. 2005.
[23] S. Boyd and L. Vandenberghe, *Convex Optimization*. Cambridge, U.K.: Cambridge Univ. Press, 2004.
[24] R. Fletcher, *Practical Methods of Optimization*. New York: Wiley, 1987.
[25] B. Cornelis, S. Doclo, T. Van den Bogaert, M. Moonen, and J. Wouters, "Analysis of localization cue preservation by Multichannel Wiener Filtering based binaural noise reduction in hearing aids," in *Proc. Eur. Signal Process. Conf. (EUSIPCO)*, Lausanne, Switzerland, Aug. 2008, vol. , B. Cornelis, S. Doclo, T. , M. Moonen, J. Wouters.

Simon Doclo (S'95–M'03) was born in Wilrijk, Belgium, in 1974. He received the M.Sc. degree in electrical engineering and the Ph.D. degree in applied sciences from the Katholieke Universiteit Leuven, Leuven, Belgium, in 1997 and 2003, respectively.

From 2003 until 2007, he was a Postdoctoral Fellow at the Electrical Engineering Department, Katholieke Universiteit Leuven, supported by the Fund for Scientific Research—Flanders. In 2005, he was a Visiting Postdoctoral Fellow at the Adaptive Systems Laboratory, McMaster University, Hamilton, ON, Canada. Currently, he is a Principal Scientist with NXP Semiconductors in the Sounds and Systems Group in Leuven, Belgium, and holds an honorary postdoctoral fellowship of the Fund for Scientific Research—Flanders. His research interests are in signal processing for acoustical applications, more specifically microphone array processing for speech enhancement and source localization, adaptive filtering, active noise control, and hearing aid processing.

Dr. Doclo received the Master Thesis Award of the Royal Flemish Society of Engineers in 1997 (with Erik De Clippel), a Best Student Paper Award at the International Workshop on Acoustic Echo and Noise Control in 2001, and the EURASIP Signal Processing Best Paper Award in 2003 (with Marc Moonen). He is a member of the IEEE Signal Processing Society Technical Committee on Audio and Electroacoustics. He has been secretary of the IEEE Benelux Signal Processing Chapter (1998–2002), and has served as a guest editor for the *EURASIP Journal on Applied Signal Processing* (2005–2006).

Marc Moonen (M'94–SM'06–F'07) received the electrical engineering degree and the Ph.D. degree in applied sciences from the Katholieke Universiteit Leuven, Leuven, Belgium, in 1986 and 1990, respectively.

Since 2004, he has been a Full Professor with the Electrical Engineering Department, Katholieke Universiteit Leuven, where he is heading a research team working in the area of numerical algorithms and signal processing for digital communications, wireless communications, DSL, and audio signal processing.

Dr. Moonen received the 1994 KU Leuven Research Council Award, the 1997 Alcatel Bell (Belgium) Award (with P. Vandaele), the 2004 Alcatel Bell (Belgium) Award (with R. Cendrillon), and was a 1997 "Laureate of the Belgium Royal Academy of Science." He received a journal best paper award from the IEEE TRANSACTIONS ON SIGNAL PROCESSING (with G. Leus) and from *Elsevier Signal Processing* (with S. Doclo). He was Chairman of the IEEE Benelux Signal Processing Chapter (1998–2002), and is currently President of the European Association for Signal Processing (EURASIP) and a member of the IEEE Signal Processing Society Technical Committee on Signal Processing for Communications. He served as Editor-in-Chief for the *EURASIP Journal on Applied Signal Processing* (2003–2005), and was a member of the editorial board of the IEEE TRANSACTIONS ON CIRCUITS AND SYSTEMS II (2002–2003), the *IEEE Signal Processing Magazine* (2003–2005), and *Integration, the VLSI Journal*. He is currently a member of the editorial board of the *EURASIP Journal on Advances in Signal Processing*, the *EURASIP Journal on Wireless Communications and Networking*, and *Signal Processing*.

Tim Van den Bogaert (M'05) was born in Kapellen, Belgium, in 1978. He received the M.Sc. degree in electrical engineering and the Ph.D. degree in applied sciences from the Katholieke Universiteit Leuven, Leuven, Belgium, in 2002 and 2008, respectively.

Currently, he is a Postdoctoral Researcher at the Laboratory for Experimental ORL, Katholieke Universiteit Leuven. His research interests are in the area of binaural signal processing for hearing aids and cochlear implants.

Jan Wouters was born in Leuven, Belgium, in 1960. He received the physics degree and the Ph.D. degree in sciences/physics from the Katholieke Universiteit Leuven, Leuven, Belgium, in 1982 and 1989, respectively.

From 1989 to 1992, he was a Research Fellow with the Belgian National Fund for Scientific Research (NFWO), Institute of Nuclear Physics (UCL Louvain-la-Neuve and KU Leuven) and at NASA Goddard Space Flight Center, Greenbelt, MD. Since 1993, he has been a Professor at the Neurosciences Department, Katholieke Universiteit Leuven. His research activities center around audiology and the auditory system and signal processing for cochlear implants and hearing aids. He is the author of 110 articles in international peer-reviewed journals and is a reviewer for several international journals.

Dr. Wouters received an Award of the Flemish Ministry in 1989, a Fullbright Award and a NATO Research Fellowship in 1992, and the 1996 Flemish VVL Speech therapy-Audiology Award. He is member of the International Collegium for Rehabilitative Audiology, a Board Member of the NAG (Dutch Acoustical Society), and is responsible for the Laboratory for Experimental ORL, Katholieke Universiteit Leuven.